Korean J. Chem. Eng., **27**(6), 1621-1645 (2010)
DOI: 10.1007/s11814-010-0402-5

INVITED REVIEW PAPER

Design of particles by spray pyrolysis and recent progress in its application

Dae Soo Jung*, Seung Bin Park*,†, and Yun Chan Kang**

*Department of Chemical and Biomolecular Engineering, Korea Advanced Institute of Science and Technology 373-1, Guseong-dong, Yuseong-gu, Daejeon 305-701, Korea
**Department of Chemical Engineering, Konkuk University, 1 Hwayang-dong, Gwangjin-gu, Seoul 143-701, Korea
(*Received 9 August 2010 • accepted 15 August 2010*)

Abstract−Spray pyrolysis is a promising aerosol process to produce "designer particles" of precisely controlled morphology with decorations on surfaces or inside particles. Need of precise control of properties has sparked researches on aerosol process that may replace conventional processes such as solid state reaction process or liquid precipitation method. However, productivity is the biggest obstacle in the development of a commercial scale process because the aerosol process is essentially operated at low particle concentration compared to liquid phase processes. In this review, by reviewing publications for the last 10 years we discuss how researchers on spray pyrolysis circumvent this inherent limitation of the aerosol process. First, the process of particle design by spray pyrolysis is introduced. Some key criteria are explained for selecting each component of spray pyrolysis: precursor, additive, carrier gas, heat source, and reactor type. Second, key contributions of major groups in Korea, Japan, Europe, and America are described. Third, some of named processes to overcome productivity of spray aerosol process are introduced. Fourth, applications of spray pyrolysis to materials related to alternative energy, environmental cleaning, information processing and display, and biomaterials are considered. Finally, future prospects of spray pyrolysis are discussed along with current standing issues for further progress of spray pyrolysis.

Key words: Spray Pyrolysis, Nanoparticle, Aerosol, Atomizer, Surface Modification

INTRODUCTION

Spray pyrolysis is a generic process for producing particles by decomposing precursor molecules at high temperature. In principle, it is similar to combustion in that liquid fuel is oxidized and produces gases and particles. The only difference is that spray pyrolysis produces useful powders, whereas combustion generates pollutant particles. A typical spray pyrolysis system is composed of a reservoir for precursor solution, droplet generator, reactor, and collection unit. Precursor solutions of aqueous or non-aqueous solvents are atomized and carried by a gas into a reactor in which droplets are evaporated and decomposed into solid particles. Nucleation and growth of monomer precursor are also involved in the process of particle formation. Electrical heating or flame provides heat for evaporation of solvent and decomposition of precursor. Some non-conventional heating methods such as microwave or laser are employed for controlling morphology.

Mass production of powders is commonly achieved by solid state reaction method in which there is sintering and grinding of precursor materials, or by heat treatment of precipitates from dissolved salt solution. However, these processes are not generally suitable for nano- or submicron size particles of precisely controlled morphology. Spray pyrolysis has its own inherent advantages over these conventional processes. Short residence time and homogeneous mixing of precursor in one droplet contribute to high purity and uniformity of phase and composition of multi-component functional powders. Application of spray pyrolysis is not limited to powder production. It covers a wide range of non-conventional applications such as preparation of field effect transistor [138,139], solid coating of refractive materials [13] and carbon nanotubes [124,125].

Spray pyrolysis technology has been used for long time in ceramic powder processing [157]. The review by Kodas and Hampden-Smith in their monograph [156] is an excellent summary of spray pyrolysis researches up to 1999. Fig. 1 is a plot of the number of papers related to "spray pyrolysis" with time. This data was obtained from the database, "web of knowledge", provided by Thomson Reuters. The total number of papers is around 4800, among which 3600 papers were published in the last 10 years. Three distinct phases are observed in this plot. The first phase is up to the late 1980's. No sig-

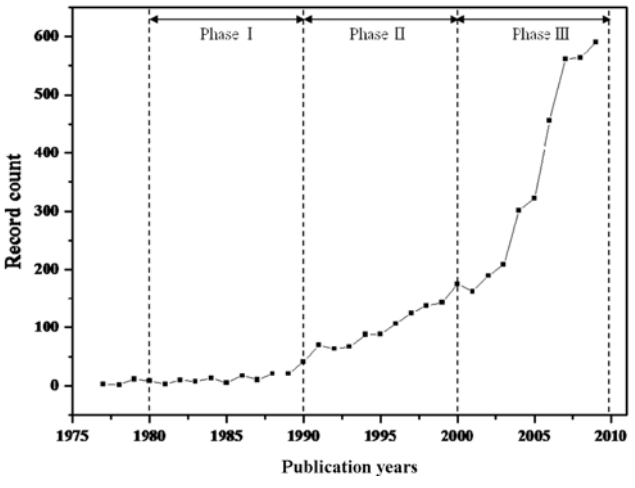

Fig. 1. Number of published papers on spray pyrolysis since 1976.

†To whom correspondence should be addressed.
E-mail: SeungBinPark@kaist.ac.kr

nificant activities are observed in this period. The second phase of research is up to the 1990's. The number of publications increases faster than in the first phase. In the 2000's, the rate of increase is more than doubled. Furthermore, there is no plateau in this plot. This means that the spray pyrolysis technology is not yet fully developed for commercial scale implementation. Delivery of full understanding on the fundamental process is required for successful engineering of the spray pyrolysis process. It also should be mentioned that spray roasting, evaporative decomposition, aerosol thermolysis, mist pyrolysis, and flame pyrolysis are essentially referring to spray pyrolysis in the literature. But the number of papers is not significant to change the statistics in Fig. 1.

The purpose of this review is two-fold: to propose a set of components to design a new spray pyrolysis after introducing some basic elements of spray pyrolysis, and to summarize recent research progress on spray pyrolysis for the last 10 years. First, we re-interpret spray pyrolysis process under the context of a strategic design of new particles and production system. A mix-and-match selection of various components of spray pyrolysis system will provide a new spray pyrolysis process which will satisfy the specification of powder for specific application. The second part is allocated to the introduction of research achievements of major groups in Korea, Japan, Europe and America. Selection of groups is done based on the frequency of appearance in the major journals, as shown in Fig. 2. It should be emphasized that the number of papers contributed from Asian countries exceeds the number of papers published by American and European countries. This statistic indicates that Asian countries, including Korea and Japan, are leading in production of and research on raw materials for electronics and information devices. The last part introduces some of the research activities from the application point of view. Especially, applications to energy, environmental clean-up, information display and processing, are to be focused.

DESIGN OF NEW SPRAY PYROLYSIS SYSTEM BY "MIX-AND-MATCH" OF COMPONENTS

Fig. 3 shows a procedure for spray pyrolysis system design in which five key steps of design are listed in sequence. The first step

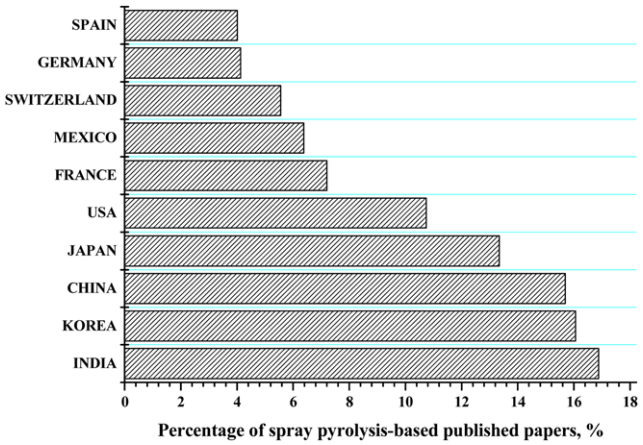

Fig. 2. Leading countries in spray pyrolysis research for the last 10 years.

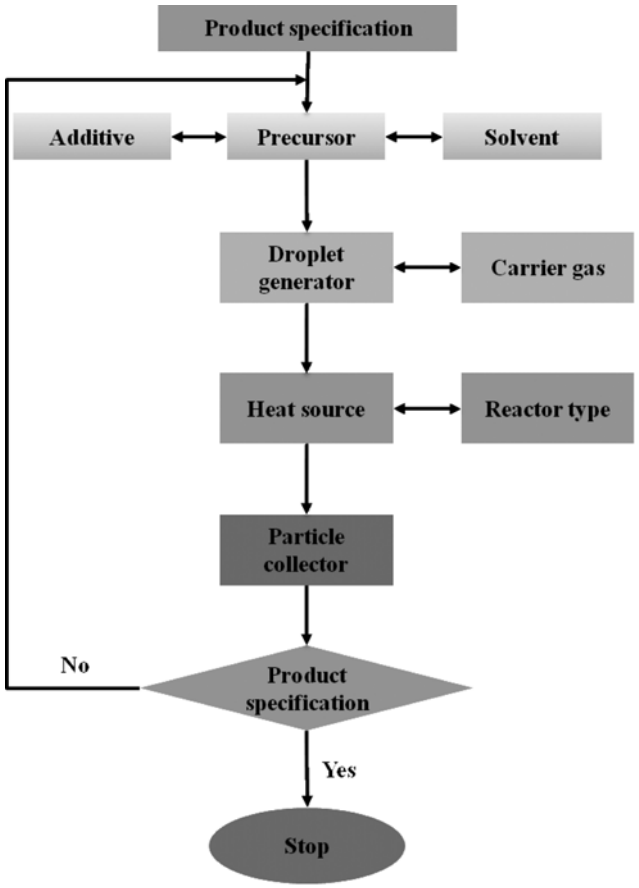

Fig. 3. Design procedure for spray pyrolysis process.

is to define product specifications. Composition and size are normally the most important properties of particles, in addition to other properties such as size distribution and morphology. Occasionally, surface properties are key properties of particles. Once the specifications are fixed, precursor and solvent are selected along with some additives which would control morphology or size of particles. The third step is to select a proper droplet generation method which is suitable for atomizing a given set of precursor and solvent. Heating method and reactor type are determined primarily based on decomposition temperature of precursor and crystallization temperature of product particles. However, morphology and particles size are affected by heating method and reactor operating conditions. Particle collectors are installed at the end of a reactor. Bag filter or electrostatic collection system are mainly used. No detailed discussion on collector part will be included in this review. If the properties of the produced particles do not meet the intended specification, further modification of reactor type or operating conditions is needed. In what follows, each step of the spray pyrolysis process will be discussed in detail.

1. Selection of Precursors

Table 1 is a summary of various types of precursors. Inorganic salts such as nitrate, carbonate, sulfate and chloride are the most commonly used precursors. Most of the single or multi-metal oxide particles are produced from inorganic salts. Key criteria of selecting precursors are solubility and decomposition temperature. Large difference of solubility of two different salt results in non-uniform

Table 1. Precursors for spray pyrolysis

Compounds	Comment	Example
Inorganic compounds	Most commonly used precursors. Solubility and decomposition temperature affect shape of particles	Nitrate [1], Carbonate [2], Sulfate, Chloride [3]
Metal-organic compounds	Improve volatility for application in AACVD and in gas-to-particle conversion	Acetate [4], Oxalate [5], Butoxide [6], Alkoxide [7], $Cu(hfac)_2$ [8]
Organometallic compounds	Improve volatility for application in AACVD and in gas-to-particle conversion	$Sn(CH_3)_4$ [9], $Al(i\text{-}Bu)_3$ [10]
Colloid	Control porosity of particles	Particulate sol [11], Polymeric sol [12], Emulsion (W/O, O/W) [13]

composition of particles because precipitation occurs at different saturation concentration. Some salts melt before they are decomposed, which makes the morphology of particles unpredictable. Inorganic salts are inexpensive and water-soluble, which are main advantages of spray pyrolysis of aqueous droplets. Impurities carried into particles from inorganic salt are occasionally serious in case of chlorides or sulfates precursors.

Metalorganic and organometallic compounds are also good precursors that make the application of spray pyrolysis more flexible. Especially, these precursors are useful for thin film formation at low temperature or high rate of production of nanoparticles. However, these precursors are unstable, toxic and relatively expensive. They are decomposed at low temperature so that particles are produced through gas-to-particle conversion process. The role of organic liquids is multiple: solvent, fuel for flame, or explosive for disintegration of particles.

Colloidal particles such as simple colloid or water-in-oil emulsion are used for porosity control of particles. Dense particles are produced when colloidal particles are precursors because, in the drying stage, no hard shell is formed so that solvent molecules are evaporated and they escape through pores easily.

2. Solvent and Additives for Spray Pyrolysis

Table 2 is a list of solvent and additives to formulate precursor solution for spray pyrolysis. Inorganic salts and metalorganics are paired with water and organics as a solvent, respectively. The key selection criteria of solvent are density, vapor pressure, viscosity, and surface tension. These properties affect droplet formation and morphology of particles. Some noble application employs ionic liquid or supercritical fluid.

The purposes for adding additives to solvent are multiple. One of the roles of an additive is to modify the physical properties of the solution itself such as viscosity or surface tension, which influences droplet size or generation rate in aerosol generators. Prevention of agglomeration is another role of additives. Aggregation-free particles are produced after salt or silica is dissolved out by water or hydrofluoric acid. Properties of particles are altered by additives. For example, sucrose or CNT's are used to control particle property such as conductivity of particles. Disintegration of a particle into primary particles of nanometer size is one of the key mechanisms to produce nanoparticles. An explosive such as urea is an additive for disintegration. One of the concerns of adding additives is contamination, which may be a serious problem depending on application of particles.

3. Droplet Generators and Carrier Gas for Spray Pyrolysis

In principle, droplets of liquid are produced by applying inertial force on a liquid stream. For efficient disintegration of a liquid stream, the inertial force exerted on the liquid should be much larger than the surface tension. A dimensionless number, Weber number, is a measure of the magnitude of relative strength of these two forces.

$$\mathrm{We}=\frac{\rho v^2 l}{\sigma} \tag{1}$$

ρ: density of liquid
v: linear velocity of liquid
l: characteristic length, typically the droplet diameter
σ: surface tension

Expansion of a pressurized liquid stream through a nozzle is the simplest form of droplet generation. The velocity of the liquid stream is limited by the nozzle diameter and thermodynamics of expan-

Table 2. Solvent and additives for spray pyrolysis

	Comment	Example	Ref.
Solvent	Viscosity, density, surface tension are key properties that affect morphology and productivity	Water	[14]
		Ionic liquids	[15]
		Supercritical fluids	[16]
		Organics	
Additive	Modification of viscosity and surface tension	Surfactants (SDS , PVP etc)	[17]
	Prevention of agglomeration	Salts (NaCl)	[18]
	Improve properties including morphology or electrical conductivity of product	Sucrose	[19]
		CNT	[20]
		Explosives (Citric acid, Urea)	[21]

Table 3. Advantages and disadvantages of various types of droplet generators

Droplet generator	Generation mechanism	Advantages	Disadvantages	Ref.
Pressure atomization	Shear force by expansion of pressurized liquid	High productivity	Large size (~50 micrometer) Hard to control size and distribution	[140]
Two-fluid atomization	Shear force exerted on liquid entrained by expansion of pressurized gas	High productivity Relatively easy to control size and size distribution	Low number concentration of droplets	[7]
Ultrasonic atomization	Shear force exerted by ultrasonic cavitations generated by piezoelectric disc	Uniform droplets with diameter less than 10 micrometer Easy to operate and construct	Not applicable to high concentration or high viscosity solution	[22]
Ultrasonic spray nozzle	Combination of pressurized expansion of liquid and ultrasonic cavitations	Stable production of droplets	Difficult to reduce droplet size	[141]
Electrospray	Additional shear force exerted by electric field formed by high bias voltage between needle and substrate surface	Charged droplets are useful for thin film and pattern formation	Low productivity Only for conducting liquid	[23]
FEAG (Filter Expansion Aerosol Generator)	Shear force exerted by pressurized two phase flow through micro channel such as frit glass filter Reactor pressure is maintained at low pressure Droplet generation rate is related to reactor pressure, diameter of filter size, pore size, and viscosity and surface tension of liquid	Easy to scale up by simply increasing filter area. Expansion into low pressure chamber provides unique opportunity of controlling morphology and size	Primitive stage of development Difficult to control the processing parameter (due to conditions of low pressure)	[17]

sion. Nominal size of droplets is in the rage of 50 micrometers in diameter and the size distribution is relatively wide. Productivity is the best among the droplet generators introduced in this section.

A two-fluid nozzle is similar to a pressurized nozzle except that the liquid is entrained into the gas stream so that the shear force exerted on the liquid is larger than in a pressurized nozzle. The droplet size is controlled by the ratio of gas and liquid. Droplet size distribution is relatively narrow.

An ultrasonic atomizer is basically the same as a home humidifier. Piezoelectric vibration exerted on the liquid generates droplets less than 10 μm in diameter. The size distribution is reasonably narrow. The number concentration in an aerosol stream is controlled independently at a fixed liquid flow rate by varying the flow rate of carrier gas. Droplet size is controlled by the vibration frequency, whereas the liquid flow rate is determined by the intensity of ultrasonic vibration. The ultrasonic atomizer is the most convenient laboratory scale droplet generator because of convenience of droplet generation control. However, piezoelectric vibration is not strong enough to produce droplets from fluid of high viscosity or high concentration of slurry.

An ultrasonic spray nozzle is a combination of pressurized nozzle and ultrasonic atomizer. At the tip of nozzle, a sonic wave generator is attached. Additional ultrasonic wave force is exerted on the pressurized liquid stream. Low frequency of ultrasonic wave favors generation of droplets from viscous liquid or slurry. Droplet size is larger than for an ultrasonic atomizer. Currently, sonic nozzles with vibration frequency of 50 kHz to 180 kHz are available. Stable production of droplets is an advantage of this generator.

The electro-spray atomizer produces much smaller droplets than does the ultrasonic atomizer. High voltage is applied between the needle and substrate. An electric field exerted on the liquid efficiently disintegrates liquid and produces droplets. The size of droplets is controlled by liquid rate and bias voltage. Low productivity and limitation to conducting liquid are major shortcomings.

A filter expansion aerosol generator is essentially a low pressure two-fluid droplet generator. In FEAG, glass frit filter is used in place of a nozzle. Micro channels in the filter provide additional surface for efficient transfer of shear force to the liquid stream. The droplet size is comparable to that of the ultrasonic atomizer.

Table 3 is a summary of droplet generators mentioned in this section.

The main role of carrier gas in spray pyrolysis is to deliver droplets into a high temperature zone, in which evaporation and chemical reaction occur including decomposition of precursor molecules. However, carrier gas can also be used as a reactant. For example, ammonia or hydrogen sulfide gases are used for particles of nitrides or sulfides.

4. Heat Source and Reactor

Once droplets are generated, solvent evaporates fast even at room temperature. Carrier gas carries droplets into a high temperature reaction zone in which solvent is evaporated almost instantaneously. Precursor concentration on the surface of droplet reaches to the supersaturated state and precipitation starts to occur from the outer shell. The precipitated precursors are decomposed. Nucleation and growth occur to form a particle subsequently.

Table 4 is a summary of heat sources used in spray pyrolysis. The electric tubular furnace is the most commonly used type of reactor. Heat transfers through the wall of the furnace by convection and radiation. The advantage of electrical heating is simplicity in construction and controllability of temperature. A multi-zone reac-

Table 4. Heat sources in spray pyrolysis

Heat sources in spray pyrolysis	
Role of heating	Heating methods
Evaporation and decomposition Nucleation and growth	Electric furnace (Wall heating) [24], Flame (LPG, H_2+O_2) [25], Microwave [26], Plasma (Atmospheric Plasma) [27], Laser (Nucleation stage) [28], UV (Nucleation stage)

tor with separated drying zone is possible [31,32]. A flame source using liquefied propane gas or hydrogen is also popular because of productivity and convenience of attaining high temperature compared with an electric furnace. However, control of flame temperature and flame zone requires some experience. Vaguely-defined reaction zone makes it difficult to model the process. These two types of reactor can be operated in horizontal [29] or vertical [30] orientation.

Nucleation and growth at the first stage of particle formation are influenced by many additional energy sources such as laser or electric field. Non-conventional heat sources such as microwave, plasma flame and UV light have been applied to spray pyrolysis for the purpose of preparing noble materials.

One standing issue in spray pyrolysis is the order of melting and decomposition of precursors. For precursors of high vapor pressure or low melting temperature, it is obvious that precursors evaporate before decomposition. But some precursors are decomposed right after precipitation. All these processes occur instantaneously and it is difficult to observe the phenomenon in-situ.

5. Product Specification

In Table 5, some examples produced by spray pyrolysis are summarized according to morphology, form of products and chemical composition. Spray pyrolysis produces particles of various morphology such as dense, hollow, meso- and micro porous, spherical and rod-like particles. Depending on the application, proper selection of precursors, additives, and heat sources is needed to produce these

Table 5. Specifications of product prepared by spray pyrolysis

	Example
Morphology	Dense [34-36], Hollow [37], Nano, Meso or micro porous [38], Spherical [39], Rod-like [40]
Form of product	Particle [41], Thin film [42], Coating (surface modification) [43]
Type of product	Oxide of single & multi component [13,14], Non-oxide such as phosphide, boride, sulfide, nitride [44], Metal [45]

Table 6. Examples of various morphologies in spray pyrolysis

		Product
Dense spherical shape	Colloid solution	$(Gd_xY_{1-x})_{(2)}O^{-3}$: Eu [34], $Ca_8Mg(SiO_4)_{(4)}Cl^{-2}$: Eu^{2+} [46], $LiFePO_4$/C [47], Y_2SiO_5 : Tb [48], Y_2O_3 : Eu [12]
	Polymer	Gd_2O_3 : Eu [35], $Li(Ni_{1/3}Co_{1/3}Mn_{1/3})O_2$ [49], (CeTb)$MgAl_{11}O_{19}$ (CTMA) [22], Y_2O_3 : Eu [50]
	DCCA*	Zn_2SiO_4 : MnBa [51], Y_2O_3 : Eu [52,53]
	Flux	(CeTb)$MgAl_{11}O_{19}$ (CTMA) [54]
Nano particles	Salt-assisted SP	Ga_2O_3, GaN [18], $Ca_{10}(PO_4)_6(OH)_2$, Hap [55], ZnO [56], $(Ba_{0.5}Sr_{0.5})TiO_3$ [57], $BaTiO_3$ [58]
	Citric acid-assisted SP	$BaTiO_3$ [59], Doped $BaTiO_3$ [60], $Ba_{1-x}La_xTiO_3$ [61], $NiFe_2O_4$ [62], $Ba_{1-x}Sr_xTiO_3$ (BST) [63], Mn_2O_3 [64], Co_3O_4 [21]
	Low-pressure SP	ZrO [65], TCO (ITO, IZO, AZO, GZO) [66], ZnO : Al [67], NiO [68]
	SiO_2-assisted SP	ZnS : Ni^{2+} [69]
	Emulsion-assisted SP	Y_2O_3 [13]
Various morphology	Coated particle	ZrO_2-coated $LiNi_{1/3}Co_{1/3}Mn_{1/3}O_2$ [70], Ru-Ni core-shell [71], Glass-coated silver [43]
	Small particle dispersed on a support	Pd/Al_2O_3 [72]
	Hollow particle	Hollow silica [37]
	Porous particle	TiN [44]
	Mesoporous particle	SiO_2 [38]

*DCCA: drying control chemical additive

particles. Spray pyrolysis is also suitable for preparing thin films and surface-modified particles. A wide range of particle composition is produced by spray pyrolysis including oxide of one component or multi-components, and non oxide such as phosphide, boride, sulfide, nitride, and metal.

These are only some examples that demonstrate the flexibility and applicability of spray pyrolysis. Once product specifications such as particle size, morphology, and chemical composition are determined, wide varieties of "designer particles" can be produced by combining elements of spray pyrolysis mentioned in the above sections.

Table 6 is a list of variation of spray pyrolysis designed to produce dense spherical particles, nanoparticles, and other morphologies. By "mix-and-match" of elements, completely new spray pyrolysis process can be designed and implemented.

MAJOR GROUPS IN SPRAY PYROLYSIS RESEARCHES

Despite the many advantages of spray pyrolysis, commercialization has been slow, and only laboratory scale research was in progress. However, there were active groups of researchers from which improvement and modification of spray pyrolysis were reported for the last 10 years. In this section, these groups are briefly reviewed and introduced. Selection of groups is based on the authors' own view and the list of groups is far from complete.

1. Spray Pyrolysis Research in Korea

Large-scale production of nanometer size particles is severely limited by productivity of bottom-up process in which vapor or gas molecules are nucleated and condensed in a reactor. A top-down process has the advantage of high productivity but control of size is difficult. Disintegration of droplets of precursor solution takes advantage of both controllability of a bottom-up process and productivity of a top-down process. Park's research group (1995) applied this principle to produce nanometer-sized particles in large quantity. They proposed a kind of low pressure spray pyrolysis system called "Filter Expansion Aerosol Generator (FEAG)". Large-sized frit glass filter was used to disperse liquid film, and expansion of liquid through this filter into low pressure chamber produced several micrometer size droplets [129,130].

Water-in-oil emulsion precursor solution was sprayed into the flame, and size-controlled particles in the range of 30 to 700 nm were produced [13]. Iron phosphide particles were also demonstrated to be produced by spray pyrolysis [137]. Multi-step spray pyrolysis was applied to the preparation of titania-coated nickel ferrite [75]. Park's group reported various applications of spray pyrolysis to the preparation of photocatalyst [73], phosphor [24], SOFC [74], and Li-ion batteries. Porous particles were also produced by spray pyrolysis [32].

Kang's research group is the most active in spray pyrolysis research, especially in transparent dielectric [77], glass frit for electrodes of display and solar cell [43], glass frit for multilayer ceramic capacitor(MLCC), low temperature ceramic capacitor (LTCC) [128] and glass ceramics [29]. Among glass synthetic processes, spray pyrolysis is unique in advantages of continuous processing and fewer steps of processing over commercial process.

Kang's group also proposed "organic-assisted spray pyrolysis" and produced nano particles such as $Ba_{1-x}Sr_xTiO_3$ (BST) [25], $BaTiO_3$ [59], doped $BaTiO_3$ [60], $NiFe_2O_4$ [62], Mn_2O_3 [64], Co_3O_4 [21]. Researches on bioceramics [76], SOFC [14,29], and lithium ion battery [79,80] are part of research scope of Kang's group.

Jang's research group specialized in flame spray pyrolysis and

Table 7. Korea research group

Synthesis	Composition	Precursor	Ref.
Spray pyrolysis Residence time: 2 s, Temp.: 1,173 K	$NaTaO_3$-C composite	$Ta(OC_2H_5)_5$, $NaNO_3$, Sucrose	[73]
Flame spray pyrolysis with emulsion (Heptane: medium phase of the w/o emulsion)	Y_2O_3 particles	$Y(NO_3)_3 \cdot 6H_2O$, Sorbitan monooleate, Dioctyl sulfosuccinate sodium salt	[13]
Flame spray pyrolysis 2,300 °C (flame's mixing cup)	$Ce_{1-x}Gd_xO_{2-x/2}$	$Ce(NO_3)_36H_2O$, $(CH_3CO_2)_3Gd_xH_2O$	[74]
Multi-step spray pyrolysis Residence time: 8 s, Temp.: 800-1,100 °C	Magnetically separable titania-coated nickel ferrite	$Fe(III)Cl_3$, $Ni(II)(C_2H_3O_2)_2 \cdot 4H_2O$, TTIP TEOS	[75]
Spray pyrolysis & FEAG Temp.: 800 °C	Modified YAG particles	Yttrium nitrate hexahydrate, Aluminum nitrate nonahydrate, Europium nitrate pentahydrate	[1]
Spray pyrolysis Residence time: 2 s, Temp.: 700-1,300 °C	Y_2O_3 : Eu	Y and Eu nitrates, Lithium chloride (Flux)	[24]
Spray pyrolysis Gas flow meter: 1 L/min, Temp.: 363 K (drying zone), 773 K (heating zone)	Mesoporous alumina particles	$Al(NO_3)_3 \cdot 9H_2O$, $Si(OC_2H_5)_4$, $(EO)_{20}$-$(PO)_{70}$-$(EO)_{20}$	[32]
Flame spray pyrolysis	Biphasic calcium phosphate ceramics	$Ca(NO_3)_24H_2O$, $(NH_4)_2HPO_4$	[76]

Table 7. Continued

Synthesis	Composition	Precursor	Ref.
High temp. spray pyrolysis Flow rate: 10 L/min, Temp.: 1,300-1,500 °C	BaO-Al_2O_3-B_2O_3-SiO_2-La_2O_3 glass ceramic	Barium carbonate, aluminum nitrate, boric acid, TEOS, lanthanum nitrate	[29]
Flame spray pyrolysis (CA-assisted)	$Ba_{1-x}Sr_xTiO_3$ (BST) powder	Barium carbonate, TTIP, strontium nitrate, citric acid (flux)	[25]
Spray pyrolysis Flow rate: 20 L/min, Temp.: 1,250 °C	Bi_2O_3-B_2O_3-ZnO-BaO-SiO_2 glass powders	Bi_2O_3, H_3BO_3, $BaCO_3$, ZnO, SiO_2	[77]
Spray pyrolysis Flow rate: 40 L/min, Temp.: 900 °C	$Tb_3Al_5O_{12}$: Ce (TAG : Ce) phosphor powders	Terbium oxide, aluminum nitrate nonahydrate, cerium nitrate hexahydrate BaF_2 (flux)	[78]
Spray pyrolysis Flow rate: 20 L/min, Temp.: 1,300-1,500 °C	Conductive silver-glass composite powders	$Ag(NO_3)$, ZnO, Bi_2O_3, H_3BO_3, $Ba(NO_3)_2$ $Al(NO_3)_3 \cdot 9H_2O$, Na_2CO_3, TEOS	[43]
Spray pyrolysis Flow rate: 30 L/min, Temp.: 800 °C	$Li_4Ti_5O_{12}$ negative powders	$LiNiO_3$, TTIP, Dimethylacetamide Citric acid (CA), Ethylene glycol (EG)	[79]
Spray pyrolysis (FEAG) Temp.: 900 °C, Reactor pressure: 60-400 torr	Al_2O_3	Aluminum nitrate, PEG 200	[17]
Spray pyrolysis Flow rate: 10 L/min, Temp.: 900 °C	$LiNi_{0.8}Co_{0.15}Mn_{0.05}O_2$	$Ni(NO_3)_2 \cdot 6H_2O$, $Co(NO_3)_2 \cdot 6H_2O$, $Mn(CH_3COO) \cdot 4H_2O$, DCCA	[80]
Spray pyrolysis Flow rate: 20 L/min, Temp.: 900 °C	$La_{0.8}Sr_{0.2}Ga_{0.8}Mg_{0.2}O_{3-\delta}$	Nitrate compounds	[14]
Spray pyrolysis Flow rate: 20 L/min, Temp.: 1,000-1,300 °C	Pb-rich PbO-SiO_2-B_2O_3-ZnO glass frits	$Pb(NO_3)_2$, TEOS, H_3BO_3, ZnO	[81]
Flame spray pyrolysis (Two fluid nozzle)	SiO_2 nano particle	Siliceous Mudstone	[82]
Flame spray pyrolysis (Ultrasonic vibrator)	TiO_2/SiO_2 nano particle	Mixture of TEOS and TTIP	[83]
Flame spray pyrolysis (Two fluid nozzle)	SiO_2 nano particle	TEOS	[7]
Flame spray pyrolysis (Ultrasonic vibrator)	TiO_2	TTIP	[84]
Flame spray pyrolysis (Ultrasonic vibrator)	ITO	Indium nitrate, Tin chloride	[85]
Flame spray pyrolysis	$SrTiO_3$: Pr^{3+}, Al^{3+}	$Sr(NO_3)_2$, TTIP, $[Al(NO_3)_3 \cdot 9H_2O$, $Pr(NO_3)_3 \cdot 6H_2O$	[86]
Flame spray pyrolysis	$LiCoO_2$	Acetate compounds of lithium and cobalt	[87]
Spray pyrolysis Carrier gas: 1 L/min Temp.: 100-1,000 °C	Silver nanoparticles	$AgNO_3$, PVP	[45]
Spray pyrolysis Carrier gas: 1 L/min, Temp.: 500-1,000 °C	Silver-silica Silica (7 nm)	Sol containing silver	[88]
Spray pyrolysis Carrier gas: 1 L/min, Temp.: 200-600 °C	Silver Nanoparticles	$AgNO_3$, Polyvinylalcohol	[89]
Spray pyrolysis Carrier gas: 1 L/min, Temp.: 500, 1,000 °C	Nickel oxide Nickel-silica nano composites	$Ni(NO_3)_2$, Silica (7 nm)	[90]
Spray pyrolysis Carrier gas: Argon (2.5 L/min) 10%H_2-90% Argon (1.25 L/min) Temp.: 300, 1,050 °C	Nickel particles	$NiCl_2 \cdot 6H_2O$	[91]

produced SiO_2 [7,82], TiO_2 [83,84], ITO [85], $SrTiO_3$ [86], and $LiCoO_2$ [87]. They have placed more emphasis on commercial application of spray pyrolysis.

Kim's research group contributed to the progress of metal particle production by spray pyrolysis with an emphasis of fundamental aspects of spray pyrolysis [45,88-91]. Table 7 is a summary of researches in Korea.

2. Spray Pyrolysis Research in Japan

Okuyama's group is one of the pioneers of spray pyrolysis in Japan. They proposed a salt-assisted spray pyrolysis in which primary particles are dispersed in a salt matrix and nanometer particles of agglomeration-free are formed after dissolution of salt [131]. They produced bioceramics [55], ZnO [56], $Ba_{0.5}Sr_{0.5}TiO_3$ [57], and $BaTiO_3$ [58]. Ga_2O_3, produced by salt-assisted spray pyrolysis, was shown to be converted into GaN nanoparticles under ammonia gas [18]. For the first time, this group proposed a usable process model at low pressure [67]. Transparent conducting oxides such as AZO, ITO, IZO, and GZO are produced by using the low pressure spray pyrolysis process. This group also worked on phosphor, MLCC, and CNT by using spray pyrolysis or flame spray pyrolysis.

Other research groups in Japan include Ogihara [113-115], Taniguchi [116,117], Inagaki [118], Ohara [119], and Soga [120] of which main interests are preparation of ceramic powders by spray pyrolysis.

Taniguchi et al. proposed a hybrid process combining spray pyrolysis and fluidized bed, and demonstrated that $LiMn_2O_4$ cathode powder was directly produced without sintering process [116]. Soga's research group produced vertically aligned CNT at 700 °C by spraying turpentine oil and ferrocene mixture with a two-fluid nozzle [120]. Table 8 is a summary of researches related with spray pyrolysis in Japan.

3. Spray Pyrolysis Research in Europe & India

Pratsinis' group is a leading research group in simulation of reac-

Table 8. Japan research group

Synthesis	Composition	Precursor	Ref.
Low-pressure spray pyrolysis Gas flow meter: 2 L/min Temp.: 600-1,000 °C	AZO, ITO, IZO, GZO	$(Zn(NO_3)_2 \cdot 6H_2O$, $ZnCl_2$, $Zn(CH_3COO) \cdot 2H_2O$ $Al(NO_3) \cdot 9H_2O$	[67]
Spray pyrolysis Gas flow meter: 2 L/min Temp.: 900 °C	hBN/MWCNT composite	hBN particles (30 nm), $Co(acac)_2$, $Pd(acac)_2$, PVP	[20,109]
Salt-assisted spray pyrolysis Gas flow meter: 2 L/min Temp.: 700-1,000 °C	GaN	$Ga(NO_3)_3 \cdot nH_2O$, LiCl	[18]
Flame spray pyrolysis	$BaTiO_3$	$(CH_3COO)_2Ba$, $TiCl_4$	[110]
Low pressure spray pyrolysis Temp.: 1,100 °C Reactor pressure: 40,80 torr	Ni, NiO	$Ni(NO_3)_2 \cdot 6H_2O$	[111]
Flame spray pyrolysis	$BaMgAl_{10}O_{17} : Eu^{2+}$ (BAM : Eu)	$Ba(NO_3)_2$, $(Al(NO_3)_3 \cdot 9H_2O$, $Mg(NO_3)_2 \cdot 6H_2O$, $Eu(NO_3)_3 \cdot 6H_2O$	[112]
Internal combustion-type spray pyrolysis Temp.: 700-1,300 °C	$LiMn_2O_4$	$LiNO_3$, $Mn(NO_3)_2 \cdot 6H_2O$	[113]
Ultrasonic spray pyrolysis Temp.: 400 °C (drying zone), 900 °C (heating zone)	$LiMn_2O_4$	$LiNO_3$, $Li(CH_3COO$), $Mn(NO_3)_2 \cdot 6H_2O$ $Mn(CH_3COO)_2 \cdot 4H_2O$	[114]
Ultrasonic spray pyrolysis Temp.: 400-1,000 °C	$Ba_2Ti_9O_{20}$	$Ba(CH_3COOH)_2$, TTIP	[115]
Spray pyrolysis and fluidized bed hybrid system	$LiMn_2O_4$	$LiNO_3$, $Mn(NO_3)_2 \cdot 6H_2O$	[116]
Spray pyrolysis and fluidized bed hybrid system	$LiM_{0.15}Mn_{1.85}O_4$	$LiNO_3$, $Mn(NO_3)_2 \cdot 6H_2O$, $Co(NO_3)_2 \cdot 6H_2O$, $Al(NO_3)_3 \cdot 9H_2O$, $Fe(NO_3)_3 \cdot 9H_2O$	[117]
Spray pyrolysis Temp.: 200-1,000 °C	NiO-samaria-doped ceria	$Ni(CH_3COO)_2 \cdot 4H_2O$, $Ce(NO_3)_3 \cdot 7.5H_2O$, Sm_2O_3	[118]
Spray pyrolysis Temp.: 200-1,000 °C	Ni-samaria-doped ceria	$Ni(CH_3COO)_2 \cdot 4H_2O$, $Ce(NO_3)_3 \cdot 7.5H_2O$, Sm_2O_3	[119]
Spray pyrolysis Temp.: 700 °C	VACNTs	Turpentine oil, ferrocene	[120]

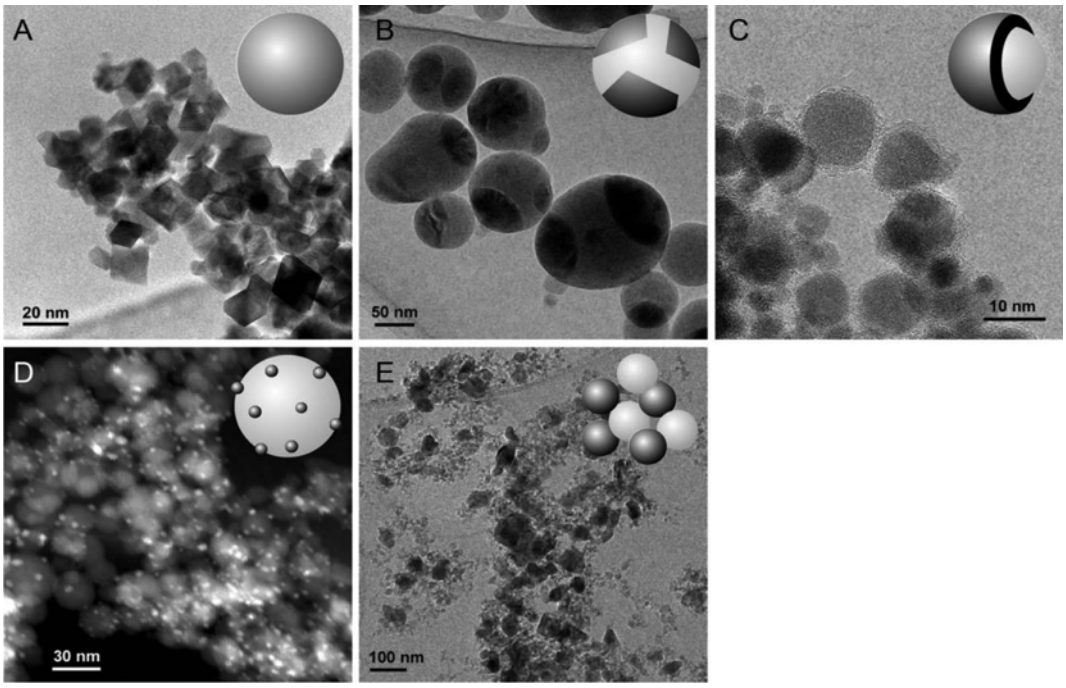

Fig. 4. Structures of multicomponent flame-made particles. A: mixed phase B: segregated phases in one particle, C: coated particles, D: small particles dispersed on a support, E: mixture of individual particles [132].

tors for particle formation in gas phase and scale-up of the reactor system. They have developed models for droplet and particle dynamics and applied to the formation of nanometer size particle of pure metal, metal oxide, mixed metal oxide. This group focuses on particle formation in flame from precursors fed as vapor and liquid. Liquid-fed flame spray pyrolysis is a versatile process that produces a wide range of particle morphology. Fig. 4 shows examples of particles produced by flame spray pyrolysis: a) mixed-oxide crystal structure, b) polycrystalline particles with two components forming individual phases within a particle, c) surface layer of one component coating the other, d) small clusters supported on the surface of the other components and e) an external mixture of separated individual particles of different components. They applied these particles to catalyst, metal-ceramic nanoparticles [95], dental materials [96], batteries [93], and phosphors [92]. Table 9 is a summary of research by Pratsinis' group. They also worked on flame spray pyrolysis as a coating process and one-step thin film formation.

Patil's group is a leading research group in obtaining high quality thin films by using spray pyrolysis in which various conditions such as substrate temperature, spray rate, concentration of solution and droplet size are investigated. Recently, they focused on preparing transparent conducting oxide films such as ZnO [98], SnO_2 [99] and doped SnO_2 [101], using spray pyrolysis, pulsed spray pyrolysis and electro-deposition processes.

4. Spray Pyrolysis Research in USA

Laine's research group mainly focused on preparation of single and mixed-metal oxide nanopowders from mixed-metal metalorganics as precursor via flame spray pyrolysis. They characterized these particles for structural, catalytic energy conversion and photonic applications. Table 10 is a summary of the group's researches. Laine et al. produced nano-sized α-Al_2O_3 powder by using liquid-fed flame spray pyrolysis. Average diameter of particles was 30-80 nm and 50-85% of alumina was transformed to α-Al_2O_3 phase. These particles are found to be densified up to 99.5% of theoretical packing density.

Suslick's group produced particles by using a sonic technology. They produced porous, hollow and ball-in-ball shape particles by spray pyrolysis. They demonstrated that hierarchically nano-structured materials are prepared by in-situ dual templating. Without using external pre-structured template, mesoporous TiN hollow microsphere was produced by nitridation of hollow Zn_2TiO_4 which was produced by spray pyrolysis [44]. They proposed a new synthetic route to produce nanostructured metal nitride of various structures. A carbon sphere was prepared from aqueous solution of substituted alkali benzoate salt. The size of the carbon sphere was controlled by precursor solution. By varying cations and ring constituents of precursor, they produced carbon powder of various morphologies such as solid sphere, hollow bowl, and porous sphere [103]. Size and morphology of the carbon sphere were demonstrated to be easily controlled in spray pyrolysis, and continuous production of carbon powder was found to be feasible by this new processing route.

CONTROL OF MORPHOLOGY IN SPRAY PYROLYSIS

1. FEAG (Filter Expansion Aerosol Generator)

Fig. 5 is a schematic diagram of a filter expansion aerosol generator (FEAG), which is a kind of low pressure spray pyrolysis system [129,130]. Characteristics of particles produced by spray pyrolysis are determined by size and size distribution of droplets. Productivity is determined by the rate of droplet generation. The ultrasonic spray generator, which is most commonly used in the laboratory, is suitable for generation of uniform-size droplets of several microns in diameter and particles of submicron size. But nanometer-size par-

Table 9. Europe & India research group

Synthesis	Composition	Precursor	Ref.
Flame spray pyrolysis	$(Y_{0.92}Eu_{0.08})_2O_3$	Nitrate compound, 2-ethylhexanoic acid (EHA)	[92]
Flame spray pyrolysis Carbon source: acetylene gas	$LiMn_2O_4$ and carbon nanocomposites	Li-acetylacetonate, Mn(III)-acetylacetonate Solvent: 2-ethylhexanoic acid, acetonitrile	[93]
Flame spray pyrolysis Carboxylic acid derived carrier liquid	Ceria/zirconia	Cerium(III) acetate hydrate, zirconium tetraacetylacetonate	[94]
Flame spray pyrolysis	Flame-made $Pd/La_2O_3/Al_2O_3$ nanoparticles	Aluminium(III) sec-butoxide, Lanthanum isopropoxide, Palladium acetylacetonate Solvent: xylene	[95]
Flame spray pyrolysis	Mixed Ta_2O_5-containing SiO_2 particles	Tantalum Butoxide, Tantalum ethoxide TEOS Solvent: Pentane, Hexane, dodecane, xylene	[96]
Flame spray pyrolysis (Organometallic solutions)	Silica-titania films	TTIP, TEOS, HMDSO	[97]
Spray pyrolysis Temp. 698 K	ZnO films	Zinc acetate Solvent: methanol	[98]
Spray pyrolysis Temp. 698 K	Tin oxide (SnO_2)	Methanolic tributyl tin acetate (TBTA) Solvent: methanol	[99]
Spray pyrolysis Temp. 573-773 K	Cadmium oxide (CdO)	Cadmium acetate Solvent: methanol	[4]
Pulsed-spray pyrolysis technique Temp. 300 °C	WO_3 films on indium doped tin oxide (ITO) coated glass	$(NH_4)_2WO_4$	[100]
Spray pyrolysis Temp. 475 °C	F : SnO_2 film	Stannic Chloride Ammonium Fluoride Solvent: methanol, ethanol, propane-2-ol and double-distilled water	[101]
Electrodeposition technique (deposited at room temperature)	nickel oxide thin films	nickel chloride	[42]

ticles are not intended to be produced by ultrasonic spray pyrolysis. FEAG was designed to improve productivity by keeping characteristics of droplets similar to ultrasonic spray generators. In FEAG, droplets of several micrometers are formed by the expansion through micro channels of glass frit field into low pressure chamber of which pressure is maintained at much less than the up-stream pressure of the filter. Fig. 6 shows the mechanism of droplet generation by the FEAG process.

Okuyama's group extended this generation unit to the production of various particles such as Ni, NiO, $BaTiO_3$ and ITO [150-152]. Jung et al. demonstrated that droplet size can be varied by controlling viscosity and surface tension of liquid and spraying pressure [17]. Gd_2O_3 : Eu phosphors were prepared by the FEAG process, with changing the mean size of droplet [147]. Mn_2O_3 and Co_2O_3 particles with fine size were prepared using the FEAG process. The prepared particles were compared with the particles prepared by ultrasonic spray pyrolysis. The particles prepared by FEAG process were finer and had more narrow size distribution and filled morphologies [148,149].

2. Emulsion-assisted Flame Spray Pyrolysis

Emulsion spray pyrolysis is another effort to improve productivity of nanometer-size particle production by spray pyrolysis. Fig. 7 is a schematic diagram of particle generation mechanism by emulsion-assisted flame spray pyrolysis [13]. Emulsion precursor (water-in-oil) is sprayed into the flame and particles are disintegrated to nanometer size because of oil burning. This mechanism is similar to disintegration of particles in FEAG. Emulsion size is controlled by the ratio of oil to water, which controls the primary particle size. Song et al. demonstrated that the primary particle size can be varied from 30 nm to 300 nm by simply varying emulsion size without controlling droplet size.

3. Organic-assisted Spray Pyrolysis

Fig. 8 is a schematic diagram of the particle formation mechanism in organic-assisted spray pyrolysis. In this mechanism, the key idea is to make the precursor powders with a more hollow structure. The organic used as additive generates a large amount of gas inside the droplet while passing through the hot zone of a reactor and makes the precursor more hollow. The hollow powders are recrystallized and turned to slightly aggregated morphology of the primary powders with a nanometer size through heat treatment. Then, the aggregated powders are easily disintegrated to nanopowders by a simple milling process [59].

Fig. 9 is SEM images of particles produced by using ethylene glycol as organic after heat treatment at between 900 °C and 1,050 °C.

Table 10. USA research group

Synthesis	Composition	Precursor	Ref.
Spray pyrolysis Carrier gas: 1 L/min, Temp.: 700 °C	$BiVO_4$	$Bi(NO_3)_3 \cdot 5H_2O$, NH_4VO_3	[33]
Spray pyrolysis Carrier gas: 1 L/min, Temp.: 900 °C $Zn_2TiO_4 \rightarrow TiN$	TiN	$Zn(NO_3)_2$ $6H_2O$, $[NH_4]_2[TiIV(OH)_2(OCH(CH_3)CO_2)_2]$	[44]
Spray pyrolysis Carrier gas: 1 L/min, Temp.: 700 °C, 1,000 °C	$ZnS : Ni^{2+}$	Zinc nitrate, thiourea, nickel nitrate, colloidal silica (23 nm)	[102]
Spray pyrolysis Carrier gas: 1 L/min (argon) Temp.: 700 °C	Carbon spheres	3,5-Dihydroxybenzoic acid, 1,3,5- benzenetricarboxylic acid, 2-chlorobenzoic acid, etc.	[103]
Spray pyrolysis	MoS_2	Colloidal silica, $(NH_4)_2MoS_4$	[11]
Liquid-feed flame spray pyrolysis (Metalloorganic precursors)	$(t\text{-}ZrO_2)_{0.54}(\delta\text{-}Al_2O_3)_{0.46}$	$N(CH_2CH_2O)_3Al$, $Zr(OH)_2(O_2CCH_2CH_3)_2$	[104]
Liquid-feed flame spray pyrolysis (Ethanol precursor solution)	$Ce_{1-x}Zr_xO_2$ Al_2O_3-$Ce_{1-x}Zr_xO_2$		[105]
Liquid-feed flame spray pyrolysis (Ethanol precursor solution)	Al_2O_3-$MgAl_2O_4$	$Mg(C_5H_7O_2)_2$, $Al[N(CH_2CH_2O)_3$, Triethanolamine, THF	[106]
Liquid-feed flame spray pyrolysis (Ethanol precursor solution)	NiO-Co_3O_4 NiO-MoO_3 NiO-CuO	$Ni(NO_3)_2 \cdot 6H_2O$ $Cu(NO_3)_2 \cdot 2.5H_2O$, $Co(NO_3)_2 \cdot 6H_2O$, $(NH_4)_6Mo_7O_24 \cdot 4H_2O$	[41]
Liquid-feed flame spray pyrolysis	$\alpha\text{-}Al_2O_3$	-	[107]
Liquid-feed flame spray pyrolysis	YAG, $Y_3Al_5O_{12}$	YCl_3, $Y(NO_3)_3 \cdot 6H_2O$, $Al(NO_3)_3 \cdot 9H_2O$, methoxyacetic acid, aluminum trisacetylacetonate, butanol, THF	[3,108]

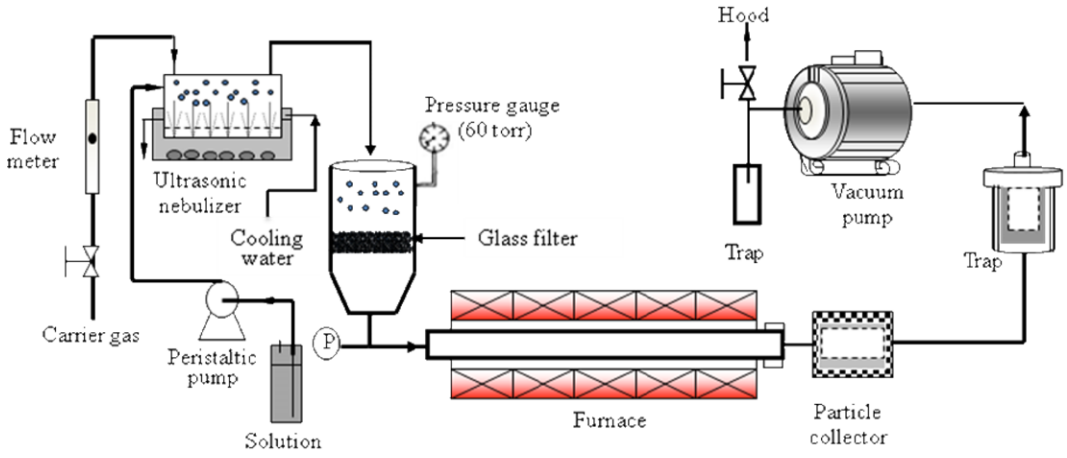

Fig. 5. The schematic diagram of FEAG process [129].

4. Salt-assisted Spray Pyrolysis

Fig 10 shows salt-assisted-spray process and schematics of particle formation mechanisms: conventional aerosol decomposition and salt-assisted aerosol decomposition [131].

Typical spray pyrolysis process produces one particle from one droplet, so it is impossible to produce nanometer-size particles without droplets of nanometer scale. In salt-assisted spray pyrolysis, the primary particles are formed within the salt matrix, and nano particles are produced through the washing process.

5. Low Pressure Spray Pyrolysis

Fig 11 is a schematic diagram of low pressure spray pyrolysis and the formation process of nano-powders. Solvent evaporates extremely fast under low pressure condition, droplets rupture and precursor monomers of ultrafine size are formed. When the temperature in the reactor is high enough to decompose precursors, oxide monomers are formed. Initially, particle size grows by the mono-

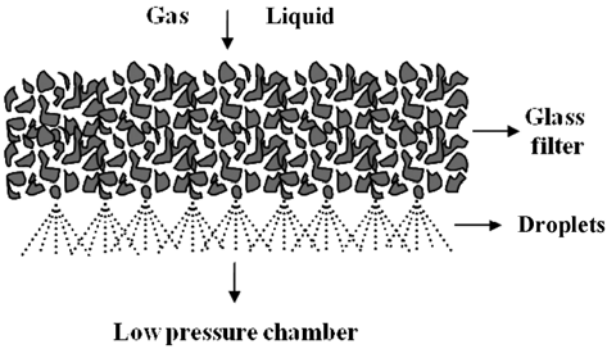

Fig. 6. The mechanism of droplets formation in FEAG [130].

mer-monomer coagulation or by nucleation. Coagulation and surface growth take over the growth mechanism in the later stage of particle growth [65].

6. Silica-assisted Spray Pyrolysis

Nanostructured mesoporous hollow microsphere can be synthesized by mixing precursor and silica particles in the tens of nanometer-size as templates and dissolving out silica with ethanolic hydrofluoric acid. Particles with high surface area are produced [69].

APPLICATIONS OF MATERIALS PREPARED BY SPRAY PYROLYSIS

Innovative materials driven from nanophase, nano-structured,

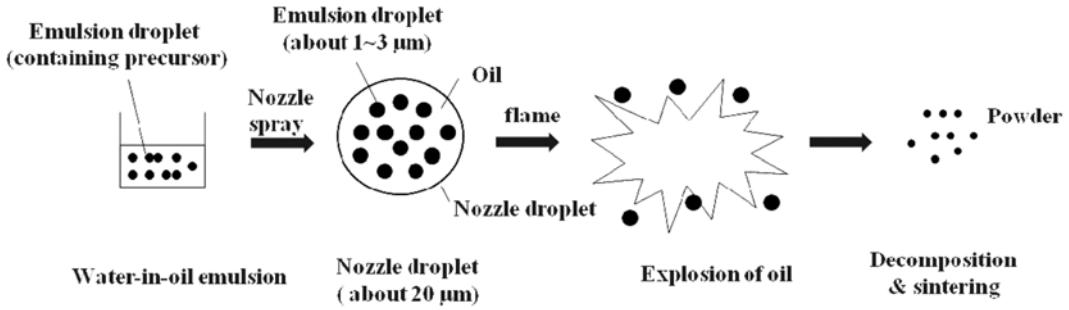

Fig. 7. A schematic diagram of the emulsion-assisted flame spray pyrolysis [13].

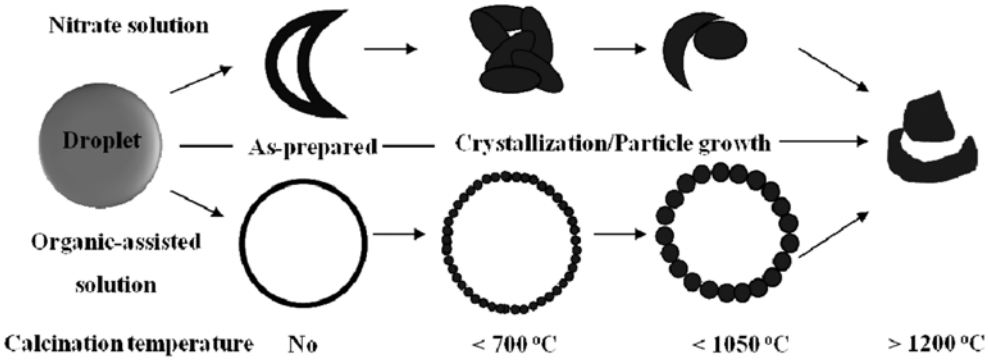

Fig. 8. Schematic diagram of organic assisted-spray pyrolysis [59].

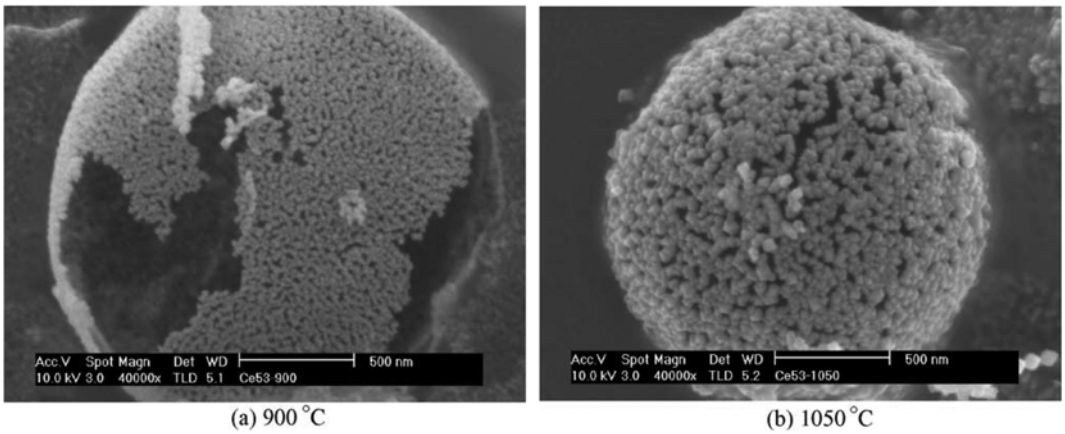

(a) 900 °C (b) 1050 °C

Fig. 9. SEM photographs of Gd-doped ceria particles prepared from ethylene glycol solution at different post-treatment temperature [122].

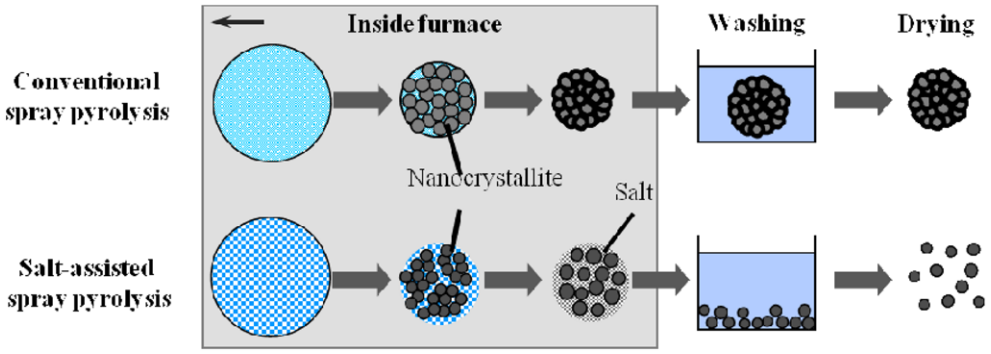

Fig. 10. Schematic diagram of salt assisted-spray pyrolysis [131].

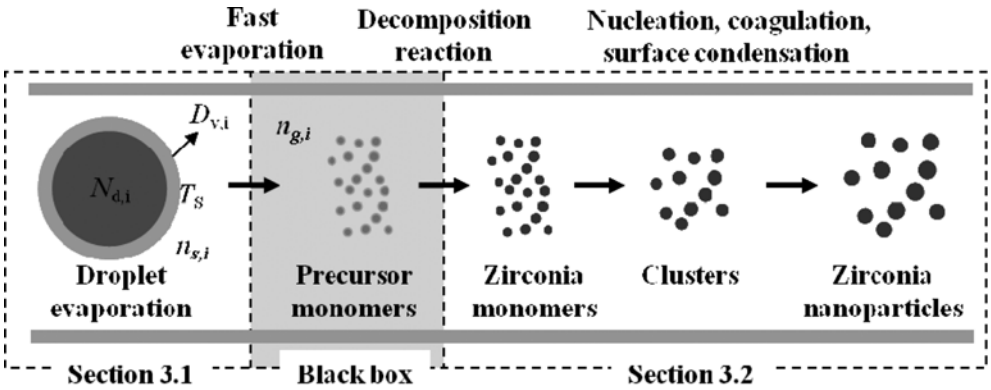

Fig. 11. Schematic diagram of low pressure spray pyrolysis [65].

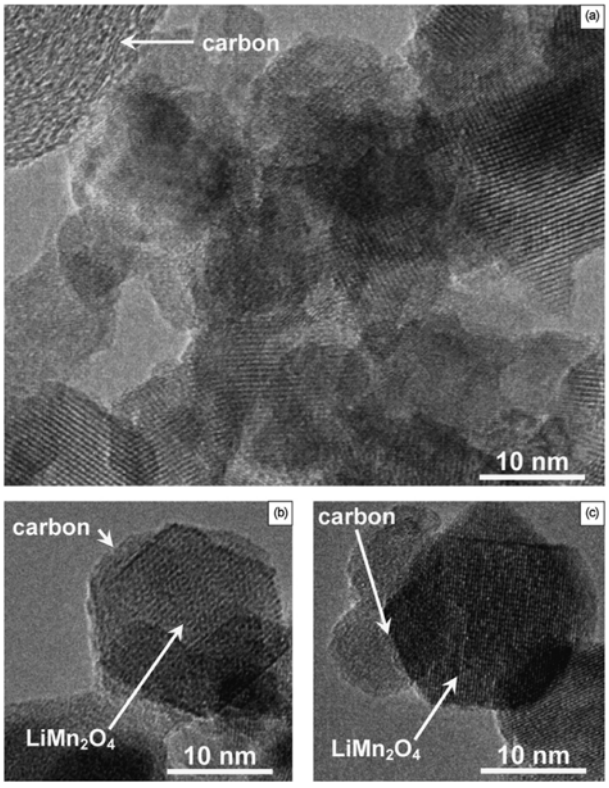

Fig. 12. TEM images of (a) $LiMn_2O_4$/carbon nanocomposites depicting (b) amorphous carbon films and (c) particles attached to $LiMn_2O_4$ crystalline particles [93].

and multifunctional materials are the major driving force in the advancement of energy, environment and health. Building blocks of these materials are, in principle, fine or nano-size particles which are transformed into films, coatings and other functional 3-D structures. In this section, materials produced by spray pyrolysis are reviewed from the point of applications to energy, environment, information display and processing, and health. References cited in this discussion are mainly from the last 10 years of publications. Advantages of spray pyrolysis over conventional processing methods are focused.

1. Energy Application of Materials Produced by Spray Pyrolysis

1-1. Electrodes for Li-ion Batteries

Conventional solid state processing and sol-gel processing have been used for preparation of electrode materials for lithium batteries. One of disadvantages of solid state processing is the long processing time for milling and mixing, which results in low productivity and possibility of inclusion of impurities. Sol-gel processing also requires a multi-step processing of mixing and drying in addition to hydrolysis and condensation of precursors. Co-precipitation includes precipitation of hydroxides, separation of precipitates, and heat treatment. However, real justification for the need of a new preparation method lies in that powders produced by different processes are not equivalent in terms of critical properties affecting battery performance. Performance of lithium batteries sensitively depends on composition, morphology, specific surface area and crystallinity of electrode materials.

Ju et al. (2010) reported spherical $Li_4Ti_5O_{12}$ powders with high density prepared by spray pyrolysis process [79]. High packing density minimizes the diffusion pathway length and results in better

performance than electrodes prepared by conventional process. They reported initial discharge capacity of 171 mAh/g at constant current density when drying control chemical additive is applied. The same preparation method was applied to the preparation of dense and spherical $LiNi_{0.8}Co_{0.15}Mn_{0.05}O_2$ cathode powders, and they reported 215 mAh/g of discharge capacity at constant current density of 0.5C [80].

Combination of diffusion flame and flame spray was applied to the preparation of $LiMn_2O_4$/carbon nano-composite [93]. Fig. 12 shows three different morphologies of $LiMn_2O_4$ particles coated with carbon particles. Improved electrical performance over simple physical mixing of active particles and carbon black was reported by Patey et al. (2009) when this composite particles prepared by spray pyrolysis are used as electrode.

Ju et al. prepared Cu-Sn alloy powder for Li-ion battery electrode under reducing atmosphere (H_2/N_2=10%/90%) by spray pyrolysis [121]. Jang et al. synthesized $LiCoO_2$ nanoparticles of 11-35 nm by flame spray pyrolysis, and cycle stability and reactivity were found to be improved [87]. Sun et al. (2005) prepared molybdenum-doped $Li[Ni_{1/3+x}Co_{1/3}Mn_{1/3}Mn_{1/3-2x}Mo_x]O_2$ with high homogeneity and high capacity [143]. The electrode has a high discharge capacity of 175 mAh/g and good capacity retention. In addition, they reported preparation of $LiNi_{0.5}Mn_{1.5}O_{4-\delta}$ with two different space groups. Structure and electrochemical characteristics were investigated [142].

1-2. Electrode for Fuel Cell

A fuel cell produces electricity by the controlled reaction of hydrogen and oxygen and is a more efficient generation system than the Carnot cycle. It has pollution-free operation, easy load leveling, availability of full range of generation capacity, and no need of electricity transmission due to on-site construction. However, full scale commercial adaptation of fuel cell is not yet near to consumer marketplaces.

Among various types of fuel cells, the solid oxide fuel cell draws the attention of researchers because of high efficiency, but commercialization of solid oxide is hindered by a high operating temperature of 600-1000 °C. The key to lowering the operating temperature is to find a new electrolyte with high ion conductivity and processing method of the electrode. Most commonly used electrolyte for solid oxide fuel cell is yttrium stabilized zirconia (YSZ) of which ionic conductivity is optimum at temperature higher than 1000 °C. Conductivity of ceria-based electrolyte is optimized at lower temperature than YSZ. However, a packing density of 95% is achieved only when it is sintered at 1600 °C at which simultaneous sintering of ceria particles and other electrode materials occurs. One of the ways to lower the sintering temperature is to prepare ultra-fine particles of ceria and additives for sintering.

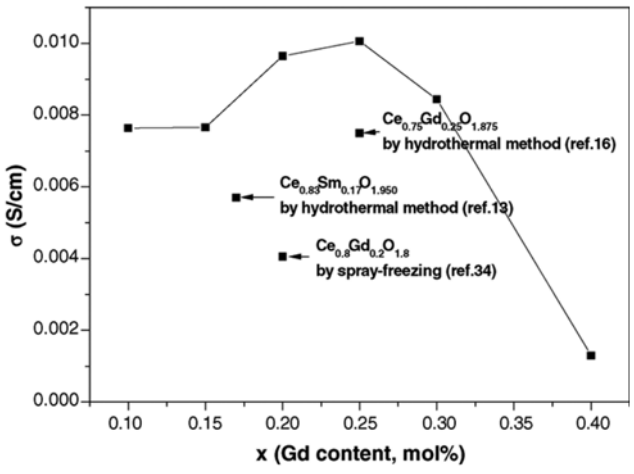

Fig. 13. Concentration dependence of the ionic conductivity of $Ce_{1-x}Gd_xO_{2-x/2}$ solid solutions at 600 °C [74].

Kang et al. (2005) reported Gd-doped ceria powder by adopting ethylene glycol and spray pyrolysis. Ethylene glycol additive produces gas during reaction and helps to form thin layers of particles, which results in small nano-size particles of 46 nm. Gd also depresses the rate of grain growth. Ionic conductivity of electrode made of Gd-doped ceria particles was comparable to YSZ [122].

Fig. 13 shows the result reported by Seo et al. (2006). They reported $Ce_{1-x}Gd_xO_{2-x/2}$ of 25 nm diameter prepared by flame spray pyrolysis. Ionic conductivity of $Ce_{1-x}Gd_xO_{2-x/2}$ (x=0.25) was 0.01 S/cm at 600 °C, which is higher ionic conductivity than particles prepared by hydrothermal synthesis.

Jung et al. (2009) reported a sealant glass powder used for planer-type solid oxide fuel cell. The sealant keeps air and fuel separated in a fuel cell [29]. Jung et al. (2009) reported $La_{0.8}Sr_{0.2}Ga_{0.8}Mg_{0.2}O_{3-\delta}$ (LSGM) prepared by spray pyrolysis. Sintered density was 95% and ionic conductivity was reported to be 2.89×10^{-3} S/cm at 500 °C, which is higher performance than that of conventionally prepared powders. This is a good example of usefulness in the preparation of multicomponent oxides [14].

For commercial scale production of PEMFCs, platinum should be replaced with low-cost materials or loading of platinum should be reduced. Thus, it is required to develop a new synthetic process to produce highly dispersed ultra-low-Pt-loaded electrocatalysts. Gamburzev et al. (2000) prepared electrocatalysts with highly dispersed Pt on carbon support by using spray generation method [154]. Suslick's research group reported carbon powder of various morphologies by spray pyrolysis. Bang et al. (2007) applied the carbon powder to direct methanol fuel cell (DMFC) for which the carbon powder is used as catalyst support and pore former in membrane electrode assembly (MEA) [145].

1-3. Photocatalyst for Hydrogen Production

Sun light is the most promising alternative energy source in the future. Conversion of sun light into electricity is already commercially available and on the verge of competing with conventional generation of electricity if the installation of photovoltaic systems keeps increasing at the current pace. Photosynthesis, a conversion of sun light into chemical energy, is the foundation of life for all plants. Mimicking photosynthesis, or artificial photosynthesis, has been on the top list of research agencies of all countries. However, no commercial scale production of chemicals from sun light has been reported. Hydrogen production from water by using photocatalyst is the closest result to the artificial photosynthesis so far. Developing new, efficient photocatalyst has been a key issue since Honda and Fujishima discovered bubbling gas from their experimental unit screening light sensitive materials for photocopy machine.

Photocatalysts are prepared by a batch process such as solid state reaction, hydrothermal method, co-precipitation method, and sonochemical method. Spray pyrolysis is a continuous process and the

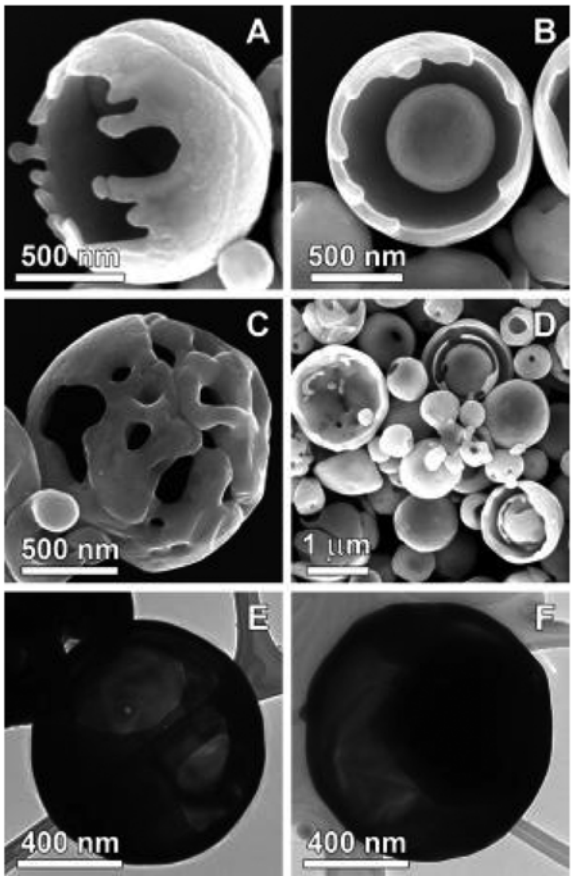

Fig. 14. SEM (A B C and D)_ and TEM (E and F) micrographs illustrating typical particle morphologies obtained by ultrasonic spray pyrolysis synthesis of $BiVO_4$ [33].

activity of spray pyrolyzed catalyst is improved over catalyst produced by conventional method. Inherently, spray pyrolysis is better for composite nanostructured catalyst [73].

The focus of photocatalyst research was developing semiconductor catalyst effective under UV light or visible light. Dunkle et al. (2009) reported $BiVO_4$ catalyst by spray pyrolysis process and proved that the catalyst is effective for producing oxygen from water. To maximize the production of oxygen, the hollow structure of the catalyst was designed to be made inside the particle by using ammonia or nitrous oxide gases. Surface area of spray pyrolyzed catalyst was 3.2 m^2/g, whereas commercial bismuth vanadate has surface area of 0.45 m^2/g. The rate of oxygen generation was 433 μmol/hr, while commercial $BiVO_4$ produced 60 μmol/hr of oxygen [33]. Hollow structures of $BiVO_4$ particles are illustrated in Fig. 14.

1-4. Application of Spray Pyrolysis to Electrode Materials in Solar Cell

Electrodes for Si-based solar cell are formed by evaporation method or screen printing method, which is a wet processing. Evaporation is best for the maximum efficiency of solar cell, but the cost of operation is expensive. Screen printing method is an economically feasible process. However, when using the screen printing process, silver paste does not penetrate deep into the electrode gap, as shown in Fig. 15, and tends to be peeled off from the solar cell surface, which reduces the total contact area and cell efficiency. This problem was solved by using glass frit as a permanent binder. Kang et al. [153] demonstrated that glass frit produced by spray pyrolysis has advantages in morphology over conventionally produced glass frit which is in irregular shapes.

Jung et al. prepared glass-silver composite by a one-step spray pyrolysis and reported that sheet resistance was improved to 3.6 μΩcm, where the resistance was 9.0 μΩcm when a conventional mixing process was applied [43]. SEM images in Fig. 16 are surface section and cross section of electrodes prepared from pure silver, conventionally-mixed silver and glass, and silver-glass composite prepared by a one-step spray pyrolysis. In Fig. 16(a), silver coating on a substrate was peeled off without melting when only silver powder was sintered at 450 °C. With the addition of glass frits of 3 wt% by conventional mixing process, silver coating was densely formed on the surface with meting because of low melting temperature of glass frit as shown in Fig. 16(b). Glass-silver composite electrode prepared by a one-step spray pyrolysis is even better than the electrode shown in Fig. 16(b).

Improved contact property and electrical performance were reported by Yi et al. (2010) when aluminum film, which was used as a backside contact, was deposited with glass frit of 0.92 μm prepared by spray pyrolysis [81].

2. Environmental Clean-up

2-1. Preparation of Catalysts by Spray Pyrolysis for Environmental Clean-up

The car manufacturing industry faces the challenge of improv-

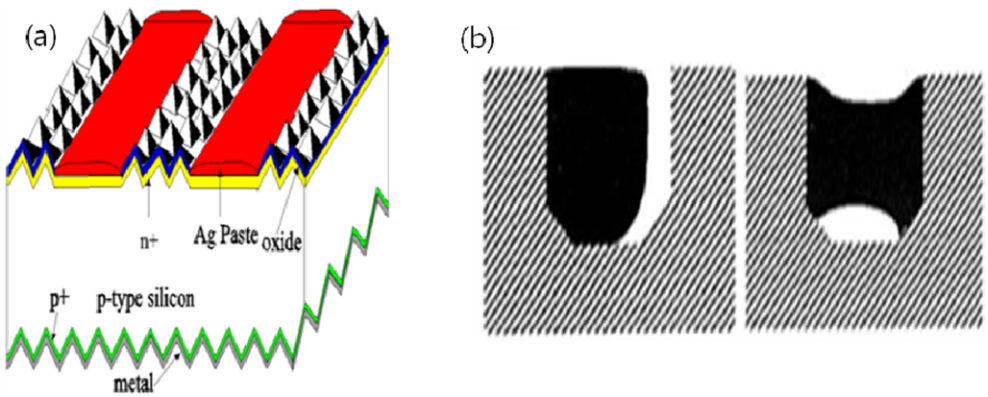

Fig. 15. (a) Schematic diagram of silicon-based solar cell and (b) screen-printed silver electrode onto Si-wafer.

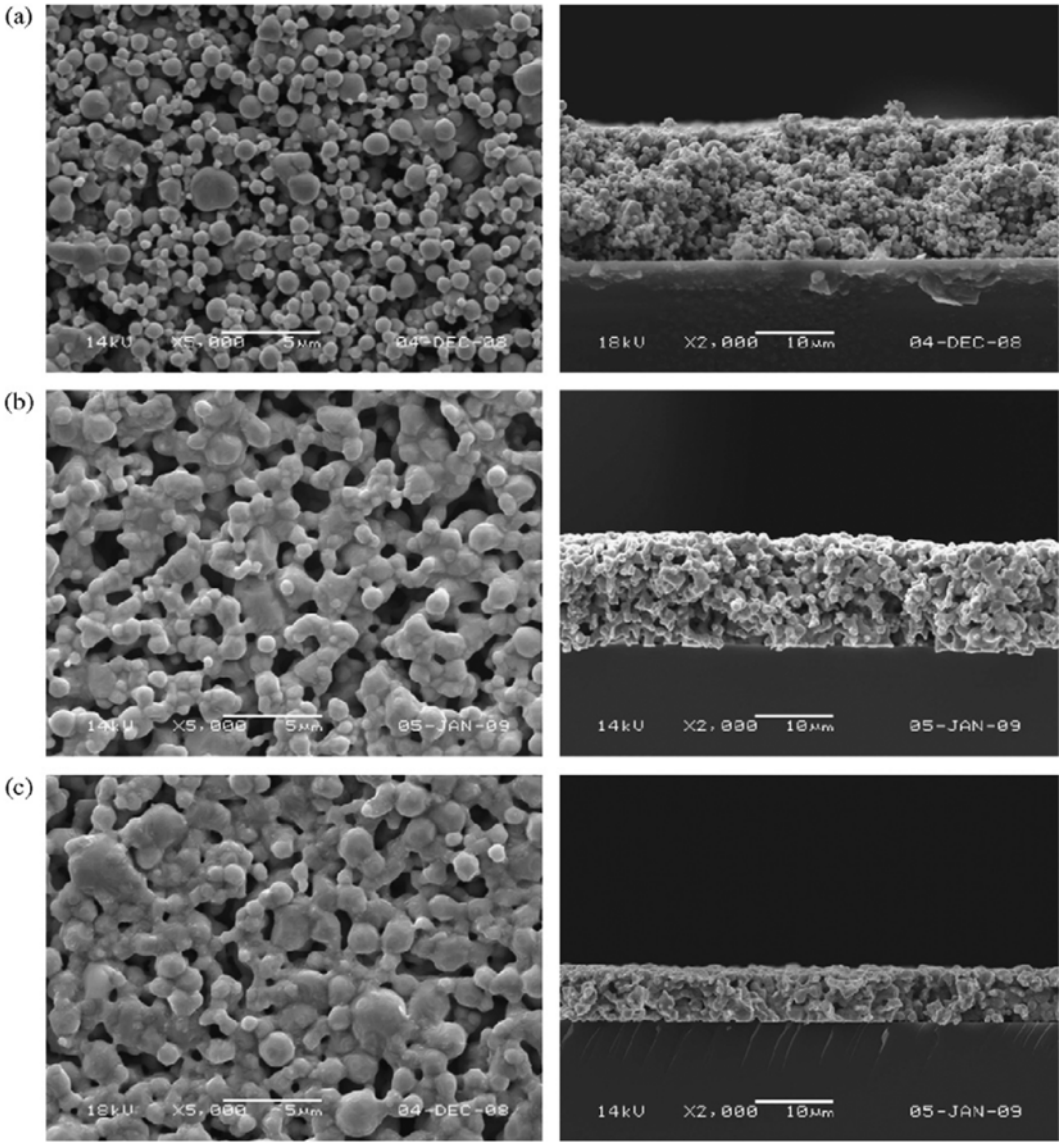

Fig. 16. SEM photographs of surfaces and cross sections of silver conducting films sintered at 450 °C (a) silver, (b) physically mixed silver and glass and (c) silver-glass composite [43].

ing fuel efficiency because of climate change caused by carbon dioxide. The automobile industry has tried a broad range of options such as two-engine technologies, lean-burn direct injection gasoline, and common turbo-diesel engines. These engines are superior in fuel economy but high air-to-fuel ratios cause the formation of high concentration of NO_x. Selective catalytic reduction of NO_x by NH_3 or hydrocarbons and nonthermal plasma method are proposed. Selective catalytic reduction of NO_x to N_2 by unburned hydrocarbons can be implemented into the current vehicle system without any engine modification.

Weidenhof et al. (2009) proposed a high-throughput screening system by using liquid feed spray pyrolysis and reported denox activity of $Ce_{1-x}Zr_xO_2$ and Al_2O_3-$Ce_{1-x}Z\ r_xO_2$ nanopowders [105].

Combustion efficiency of methane gas can be improved by catalyst such as palladium impregnated alumina. However, deactivation is a serious problem because of sintering of palladium and phase transformation. Strobel et al. (2004) prepared palladium nanoparticles (<5 nm) supported on lanthanum-stabilized alumina by flame spray pyrolysis. The surface area of the catalyst was 50-180 m^2/g, and deactivation was not serious between 700 °C and 1200 °C compared with commercial catalyst. The addition of lanthanum delayed phase transformation of alumina from γ phase to α phase at 1200 °C. Temperature required achieving 20% conversion of methane remains within a reasonable range after cycle test, which indicates that the deactivation of catalyst is not serious [95].

2-2. Control of Hydrophilicity

Superhydrophilicity of titania film appears under UV radiation and it becomes effective for anti-fogging. But under normal sunlight, superhydrophilicity does not appear. Tricoli et al. (2009) reported antifogging titania film under sun light. They prepared SiO_2-TiO_2 film by combining chemical vapor deposition and flame deposition. Silica film interwoven nanofiber or nanowire, of which size is 10-15 nm in diameter and several hundred nanometer long in length, is prepared by chemical vapor deposition. Nanoparticles of 3-5 nano-

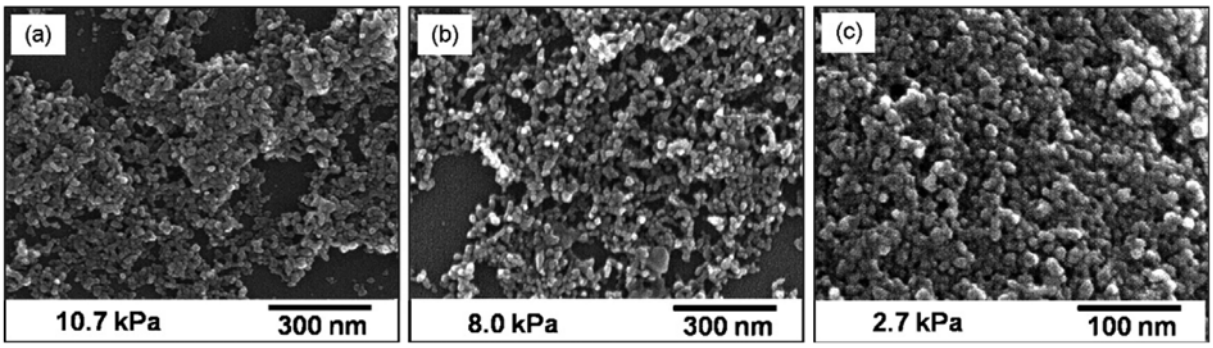

Fig. 17. FE-SEM images of LPSP-made AZO particles prepared using zinc acetate precursor $Zn(CH_3COO)_2 \cdot 2H_2O$ at various pressures of 10.7 (a), 8.0 (b) and 2.7 kPa (c) and a fixed conditions of concentration 0.5 mol/l and temperature 800 °C [67].

meters in diameter are deposited on top of this silica film by flame deposition. This film is annealed in-situ under flame. Antifogging effect under normal sun light was most effective when 40 mol% of silica was incorporated into silica-titania film [97].

3. Information Processing and Display

3-1. TCO (Transparent Conductive Oxide)

Transparent conducting oxide (TCO) is an essential material for electronic devices such as liquid crystal display, silicon solar cell, and energy windows. Hidayat et al. (2008) prepared aluminum-doped zinc oxide (AZO) particles of 16-20 nm in diameter by using filter expansion aerosol generator at 2.7-10.7 kPa. FE-SEM images in Fig. 17 show the morphology of AZO particles prepared from zinc acetate and aluminum nitrate precursors. Evaporation rate of solvent is accelerated at low pressure condition, as indicated in Fig. 11, and promotes disintegration of dried precursors, which results in particle formation of nanometer size. AZO thin film of 250 nm thickness was dip-coated and heat-treated at 400 °C for 1.5 hr. Transmittance of 400-800 nm wavelength was higher than 97% and resistivity was 4.0×10^3 Ωcm [67].

Jang et al. (2006) prepared indium-tin oxide (ITO) thin film by mixing polymer binder and nanoparticles of 11-20 nm in diameter produced by using flame spray pyrolysis. Transmittance was decreased from 92% to 83% as the particle size increased. Surface resistance was decreased from 1.0×10^4 to 0.8×10^4 Ω/□ [85].

Direct preparation of TCO film by using spray pyrolysis has the advantage of simplification of process over multi-step preparation- and coating method. Lokhande et al. (2002) prepared zinc oxide film on glass substrate directly from methanolic solution of zinc acetate. Band gap energy, electrical resistivity and thermoelectric power were found to be affected by solution concentration [98]. For the first time, Rim et al. applied spray pyrolysis method to the preparation of p-type transparent conducting oxide, copper aluminum oxide, in delafossite phase [155].

3-2. MLCC (Multi-layer Ceramic Capacitor)

Conventionally, barium titanate particles of ultrafine size with narrow size distribution are produced by liquid phase processing such as precipitation, hydrothermal process and sol-gel process. Precipitation or hydrothermal process has advantages of high purity and narrow size distribution over solid state process. However, it requires additional post heat treatment and ball milling. Sol-gel processing includes hydrolysis and condensation of alkoxides, which are toxic expensive and difficult to handle although processing temperature is low and homogeneity is excellent.

Miniaturization of electronic components sparked the need of raw materials of small particles. Especially, the multi-layer ceramic capacitor (MLCC) draws attention. Preparation of ultrafine-size barium titanate with tetragonal structure has been a key issue because the crystal structure is transformed from tetragonal to cubic as the particle size gets smaller. In practice, the crystal structure changes when the particle diameter is smaller than 50 nm, although the critical diameter for transformation is 16 nm [144].

Terashi et al. (2008) produced $BaTiO_3$ nanoparticles of high tet-

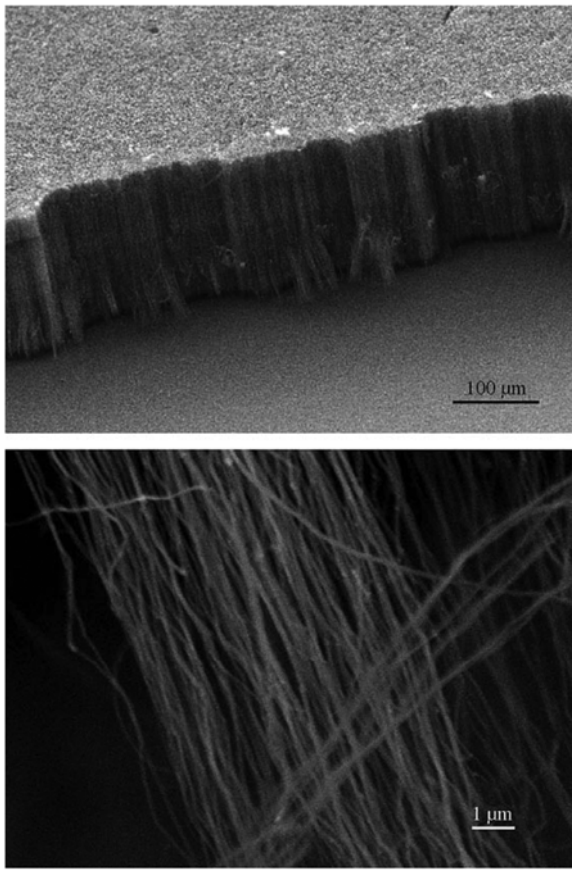

Fig. 18. CNTs formed by spray pyrolysis at 900 °C under argon flow of 4 lpm, ferrocene concentration on benzene of 18.7 g/L during 10 min of solution spraying [125].

ragonality by a one-step flame spray pyrolysis. Urea additive disintegrated submicron particles into nanometer particles. Tetragonality was increased from 1.0051 to 1.0071 with the increase of additive [110].

Miniaturization of MLCC also requires nanometer-size nickel particles which are used as an electrode of MLCC. Xia et al. (2001) synthesized nickel particles by using formic acid as reducing agent at 600 °C with residence time of 0.1 sec [123]. Wang et al. (2004) produced nickel particles of 35 nm in diameter from $Ni(NO_3)_2 \cdot 6H_2O$ by using low pressure spray pyrolysis [134].

3-3. Carbon Nanotube

Carbon nanotubes (CNTs) have excellent mechanical, thermal, electrical properties and have been produced by arc discharge, laser ablation, chemical vapor deposition and spray pyrolysis.

Khatri et al. (2009) reported successful production of single-walled carbon nanotubes (SWCNTs) at 850°C on silicon substrate from ethanol and bimetallic catalyst of cobalt and molybdenum acetates by using ultrasonic spray pyrolysis. They demonstrated that SWCNT are produced under nitrogen environment without using hydrogen as a reducing agent. This process is one of the simple and cheap alternatives for CNT production [124]. Elguezabal et al. (2006) applied spray pyrolysis to the production of multi-walled carbon nanotubes (MWCNTs), shown in Fig. 18, from ferrocene/benzene under argon flow. They reported that the diameter of multi-walled carbon nanotubes (MWCNTs) is influenced by droplet size and the length is controlled by ferrocene concentration and argon flow rate [125].

3-4. Sensors

Sensors are essential components of process monitoring and safety system. Semi-conducting gas sensors such as tin oxide and titanium-based materials were directly deposited and annealed by a one-step flame process. Fig. 19 is a schematic diagram of conventional wet-chemical technique and direct flame deposition process. Direct coating process reduced the number of processing steps so that the probability of contamination was dramatically reduced. Sahm et al. (2004) demonstrated that highly crystalline SnO_2, deposited on Pt interdigitated alumina substrate by using flame spray pyrolysis, is sensitive to NO_2 and propanal, and response time is very short [133].

3-5. Phosphors for Display and LED

Phosphor materials are used in fluorescence lamp, LED and display devices. Conventional solid state reaction method has been used to produce these phosphors. Solid state reaction method requires high reaction temperature and long heating time. Control of size and morphology is difficult for multicomponent phosphor of high purity. Milling process is vulnerable to contamination, which reduces brightness of phosphor.

Inorganic phosphors used in plasma display require uniform size distribution and spherical shape for high luminescence efficiency. Surface characteristics are also key factors for high performance phosphors because ultraviolet light penetrates only down to 10-100 nanometer deep. Currently, particles of 1-5 μm are known to be optimum for coating on display panel.

Research on preparation of inorganic phosphors by using spray pyrolysis process has been visible because of advantages in size controllability and low contamination of spray pyrolysis process. Major applications of spray-pyrolyzed phosphors are the plasma display panel, field emission display and light emitting diode.

Spray pyrolysis produces spherical phosphor particles with high crystallinity and phase purity, which are beneficial for high packaging density and improved surface uniformity. Thus, the photoluminescence (PL) intensity of phosphor can be optimized. Therefore, the spray pyrolysis method is considered as a successful candidate for the production of phosphor particles in large scale, compared with the conventional solid-state process.

Recently, white LED has drawn attention because of low power consumption and the possibility of replacing conventional fluores-

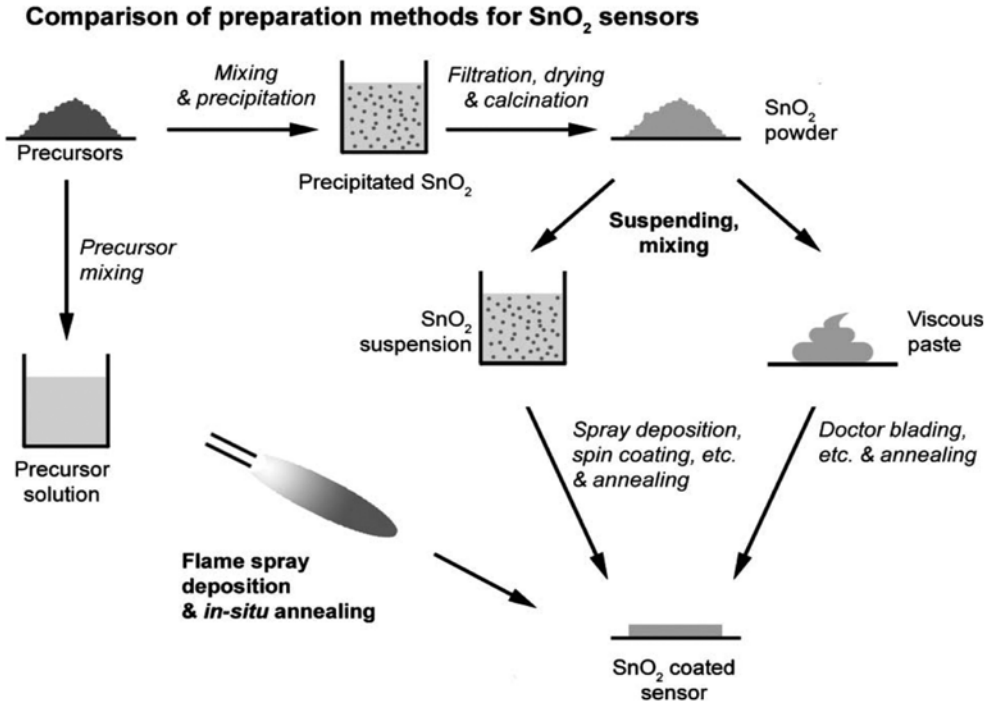

Fig. 19. Process diagram for preparation of SnO_2 gas sensors comparing wet-chemical routes and direct flame deposition [132].

cence lamps. White LED emits white light by exciting yellowish green phosphor YAG : Ce with blue light-emitting diode. If UV-emitting diode is used, the efficiency of LED will be improved. However, there are some standing issues for commercial scale production of white LED by using UV LED. Key issues are optimization of luminescence by controlling morphology and particle size distribution, thermal and chemical stability of phosphor under UV light, and controlling UV emission characteristics [136,146]. Lee et al. (2005) reported $Y_3Al_5O_{12}$: Ce phosphor particles of 1.73 μm in diameter by using spray pyrolysis. PL intensity was as good as commercial phosphor when 9 wt% of BaF_2 was added as flux [92]. Spray pyrolysis will provide a new opportunity to produce phosphor particles of uniform and ultrafine size, which will improve the quality of white LED when UV light emitting diode is used.

3-6. Glass Frit

Glass frit serves as a permanent binder, promotes the sintering of metal powders during firing, and enhances the adhesion of the film to the substrate for metallic electrodes. Also, the glass frit is used as sealant material in SOFCs and to lower the melting temperature of ceramic materials which leads to high density.

Glass frit helps to reduce electrode resistance and improve adhesion by preventing island formation in metal particles during short sintering time. Demand for electrode materials for photon harvesting devices has gradually shifted to silver, aluminum and nickel of nanometer size. Glass frit of nanometer size is also needed accordingly. Glass frit is produced by repeated melting at high temperature, rapid cooling, and milling. This process produces the irregular shape of micron-size particles.

Nano-sized glass frit was produced by plasma process and tested as electrode material. However, the plasma process requires high consumption of energy for evaporation. Instability of plasma makes it difficult to produce nano-size glass frit of controlled size. Possibilities of applying spray pyrolysis process to produce glass frit of nano-size and spherical glass were explored by Kang's research group.

Commercially, glass frits are prepared by a melting-quenching process. The commercial process has many operation steps to prepare fine glass frits, as shown in Fig. 20. The mixed powders of the reactants are ball-milled and melted in a platinum crucible at a

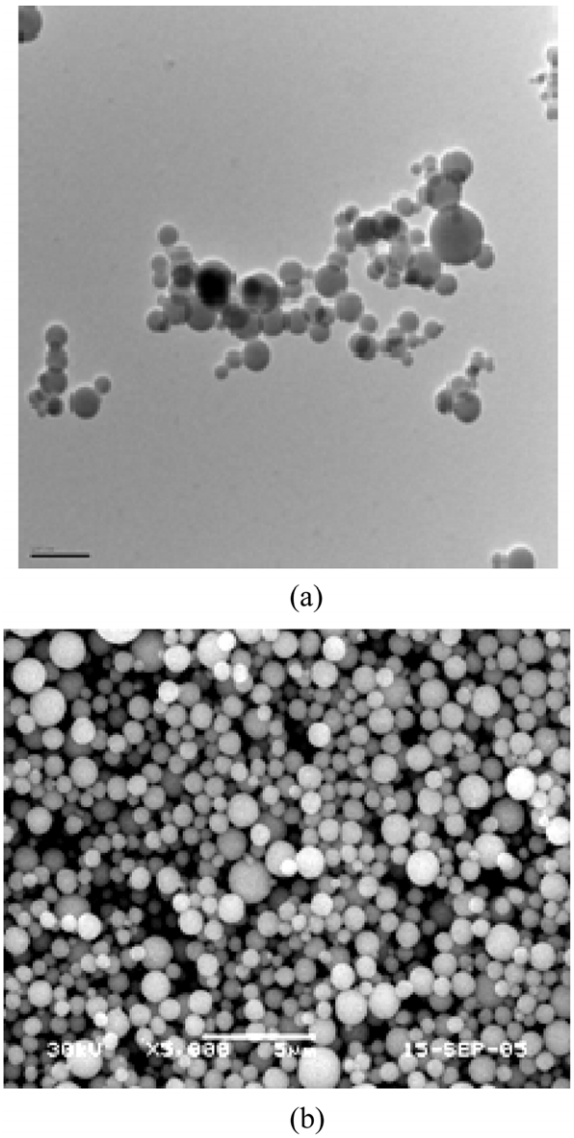

Fig. 21. TEM and SEM images of (a) nano-sized and (b) submicron sized glass powders prepared by spray pyrolysis [39, 77].

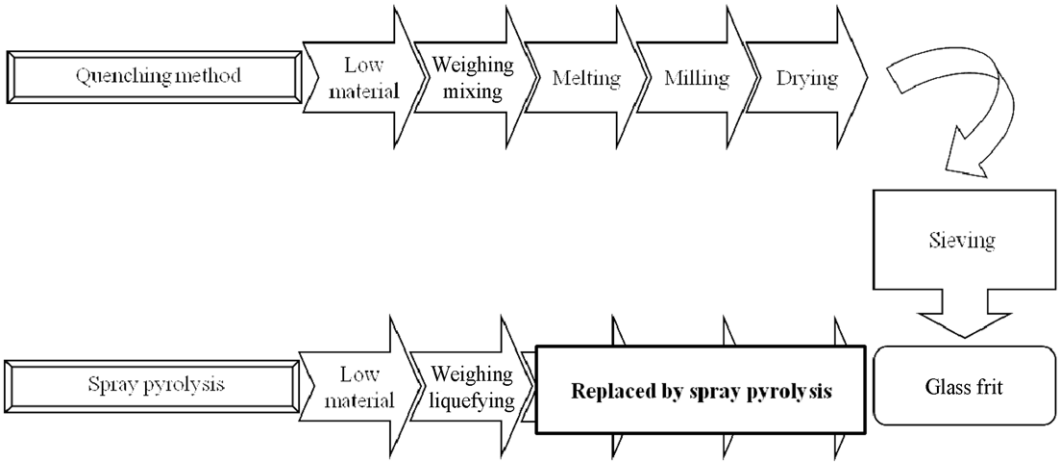

Fig. 20. Conventional melting process and spray pyrolysis process for preparing glass frit.

high temperature. Molten glasses are quenched to make glass flakes which are ground by milling process to obtain fine glass frits. However, the glass frits obtained by commercial process have irregular shape and large size. It can be difficult to reduce the size of frits under submicron size and the morphology cannot be controlled.

Spray pyrolysis has been a promising process for the preparation of improved ceramic and metal powders. Recently, glass frits were also prepared by spray pyrolysis even at short residence time of glass frits inside the reactor as several seconds which can reduce synthetic processes. The prepared glass frits controlled the frit size from micron to nanometer as shown in Fig. 21 and had spherical shape and non-aggregation characteristics. The prepared glass frits had also narrow size distribution even without milling and sieving process.

Koo et al. (2010) produced Pb-based glass powder and coated in-situ on nano silver particle by flame spray pyrolysis. This coated silver powder was sintered and tested. Fig. 22 shows the morphology of particles and electrode. The mean size of coated powders was around 42 nm, and the thickness of glass layer covering the silver powder was l.4 nm. The sheet resistivity of the electrode formed from the coated silver powders was 19 mΩ/sq at a firing temperature of 600 °C.

Transparent dielectric, $PbO-B_2O_3-SiO_2$ and $Bi_2O_3-B_2O_3-ZnO-BaO-SiO_2$ glass frit, were produced by spray pyrolysis, and performance was compared with commercial powder [77]. The dielectric layers formed from the spherical and fine-sized glass frits had a high transparency, smooth surface and no void inside the layer. However, the dielectric layers formed from the commercial glass frits had some voids inside due to their irregular shape and broad size distribution, which results in a decrease of transparency.

3-7. Preparation of Field Effect Transistor (FET) by Spray Pyrolysis

Spray pyrolysis has been mainly used for preparing particles and films. Novel application of spray pyrolysis was reported by a group from Imperial College, London. They prepared ZnO thin film at low temperature by spray pyrolysis and tested the possibility of thin film transistor. Resistance of zinc oxide varied depending on oxygen content, which makes it possible to control film property. The transparent zinc oxide can be used for transparent display. However, pure zinc oxide without dopant is not air-stable when it is exposed to air for a long period of time. Variation of zinc and oxygen stoichiometry affects electrical property. Dopants such as Al, Ga, and In are tested to improve electrical conductivity, service life and stability under long exposure to air.

Bashir et al. (2009) demonstrated that spray pyrolysis can be applied to the fabrication of high mobility and low voltage ZnO transistor fabrication [138]. Wöbkenbery et al. (2010) prepared TiO_2 thin film transistor at ambient pressure. Maximum mobility value was reported as 0.05 cm^2/V at optimized conditions. The transistor was also reported to be air-stable for several months.

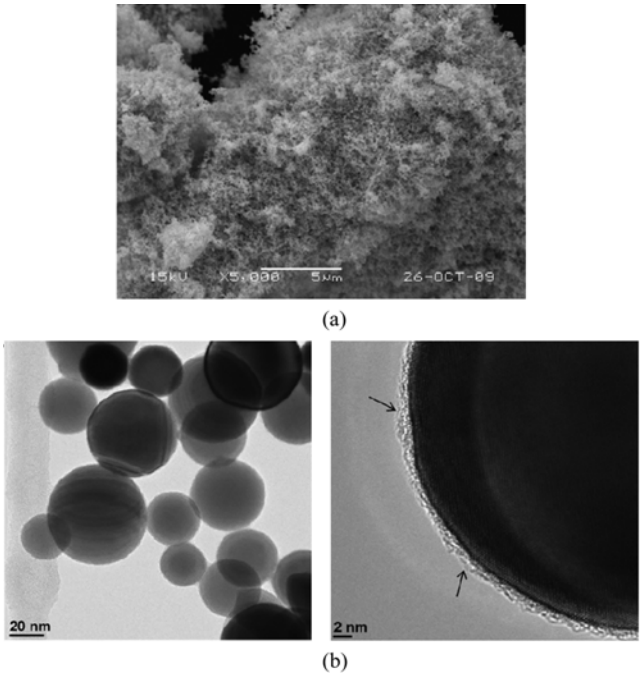

Fig. 22. (a) SEM and (b) TEM images of the nano-sized silver-glass composite powders prepared by flame spray pyrolysis [158].

4. Bio-ceramics

Another noble application of spray pyrolysis is the preparation of biomaterials such as hydroxyapatite (Hap) and tricalcium phosphate. These calcium phosphate are biocompatible and osteoconductive so that they are used for bone or tooth repair, coating for metallic implant, and bone space filler. Bioceramics are produced by various conventional techniques such as precipitation, sol-gel process, hydrothermal process, and solid state reaction method.

Solid-state reaction method requires long heat treatment, which causes sintering and reduces surface area. Liquid phase preparation needs precise control of pH and temperature. Post-processing steps such as washing, drying, and calcination are time consuming and cost-intensive. Need for complex morphology and composition is getting more important. Spray pyrolysis is one of the new feasible methods for the production of complex composition. Cho et al. (2010) prepared biphasic calcium phosphate of 35 nm by flame spray pyrolysis.

Organic monomers and ceramics filler particles were proposed and tested as a dental filling [96]. Bone defects are repaired by using calcium phosphate [76]. Core-shell structured particles of magnetic and luminescent properties are reported to be prepared by spray pyrolysis [127].

SUMMARY AND FUTURE PERSPECTIVE

Spray pyrolysis is a promising aerosol process to produce "designer particles" of precisely controlled morphology with decorations on surface or inside particles. However, commercial application of spray pyrolysis has been slow and it has failed to draw attention from companies except Degussa, Dupont and Cabot. Dupont was successful in the production of silver paste for plasma display panel in collaboration with SMP company.

To improve the performance and functionality of electronic and energy devices such as lithium ion batteries or solar cells, materials should satisfy more stringent specifications of raw materials than conventional counterpart. Need of precise control of properties sparked researches on new process that may replace conventional processes such as solid state reaction process or liquid precipitation method. However, productivity is the biggest obstacle to the development of a commercial scale process because the aerosol process is essen-

Table 11. Application

	Application	Composition	Conclusion	Ref.
Energy	Battery	$LiNi_{0.5}Mn_{1.5}O_{4-\delta}$	Synthesis of cathode materials with two different structures ($Fd^{-}3m$ and $P4332$)	[142]
		$Li[Ni_{1/3+x}Co_{1/3}Mn_{1/3}Mn_{1/3-2x}Mo_x]O_2$	Discharge capacity (x=0.01): 175 mAh g^{-1}	[143]
		$Li_4Ti_5O_{12}$ negative Powders(Li-ion)	Initial discharge capacities: 171 mAh/g (at a constant current density of 0.17 mA/g)	[79]
		$LiNi_{0.8}Co_{0.15}Mn_{0.05}O_2$ Cathode (Li-ion)	215 mAh /g (at a temperature of 55 °C under a constant current density of 0.5C)	[80]
		$LiMn_2O_4$ and carbon nanocomposites	$LiMn_2O_4$/carbon nanocomposites: >80% of initial galvanostatic discharge capacity (5~50C-rate)	[93]
		Cu_6Sn_5 alloy	Discharge capacities: dropped from 485 to 313 $mAhg^{-1}$ by the 20th cycle at a current density of 0.1 C	[121]
		$LiCoO_2$ nano particles	Average particle size: 11-35 nm	[87]
	Fuel cell	Gd-doped CeO_2	Mean size of GDC: 46 nm (Calcination temp. 1,050 °C)	[122]
		$Ce_{1-x}Gd_xO_{2-x/2}$	Ionic conductivity: 1.01×10^{-2} S/cm at 600 °C	[74]
		BaO-Al_2O_3-B_2O_3-SiO_2-La_2O_3 glass ceramic (sealant in SOFCs)	Densification of the specimen: start at a sintering temperature of 600 °C	[29]
		$La_{0.8}Sr_{0.2}Ga_{0.8}Mg_{0.2}O_{3-\delta}$ (electrolyte in SOFC)	Mean particle size of the LSGM powders: 0.89 μm Total conductivity: 2.89×10^3 S/cm (Sintering temp. 1400 °C, density: 95%)	[14]
		Porous carbon support	Demonstration of the importance of pore structure at both the cathode and anode in the development of efficient self-breathing direct methanol fuel cells	[145]
	Photocatalyst	$BiVO_4$	Hollow and porous shells structure, Ball-in-ball type structure (active for O_2 evolution under visible-light irradiation in $AgNO_3$ solution than commercial $BiVO_4$ and WO_3 powders)	[33]
	Solar cell	Conductive silver-glass composite powders (electrode)	Preparation of glass-coated silver powders (core-shell structure) Specific resistance: 3.6μΩ·cm (firing temp. 450 °C)	[43]
		Pb-rich PbO-SiO_2-B_2O_3-ZnO glass frits (Inorganic binder for Al electrode)	Glass transition temperature (T_g): 328.5 °C Mean diameter: 0.92 μm Sheet resistances of Al films: 10.8 m/sq	[81]
Environment	Catalysts	$Ce_{1-x}Zr_xO_2$ Al_2O_3-$Ce_{1-x}Zr_xO_2$	High-Throughput Screening $Ce_{1-x}Zr_{-}O_2$ and Al_2O_3-$Ce_{1-x}Zr_{-}O_2$ nanopowders (good activities for both NO_{-} reduction and propane/propene oxidation)	[105]
		$Pd/La_2O_3/Al_2O_3$ nanoparticles	Palladium nanoparticles (<5 nm) supported on lanthanum-stabilized alumina 50-180 m^2/g Excellent thermal stability in terms of specific surface area up to 1200 °C (retarded c- to a-alumina transformation)	[95]
	Anti-forgging	Silica-titania films	Prepared films (300 nm): completely prevented fogging of the glass substrates	[97]

Table 11. Continued

	Application	Composition	Conclusion	Ref.
Information process & display	TCO	ZnO films	Bandgap energy: 3.33-3.24 eV Room temperature electrical resistivity: 10^{-2}-10^{-3} Ω cm	[98]
		AZO, ITO, IZO, GZO	Particle size: 16-20 nm, Transmittance >97% Resistivity: 4.0×10^{3} ohm cm	[67]
		ITO	20 nm, Spherical, Transparency: 92% Surface resistance: 0.8×10^{4} Ω/ □	[85]
		$CuAlO_2$	Show 3 times higher than that prepared by the solid state reaction	[147]
	MLCC	$BaTiO_3$	Particle size: 23-33 nm, High tetragonality: 1.0071	[110]
		Nickel powder	Preparation of agglomerated nanoparticles, nonagglomerated submicrometer particles, hollow particles, and spherical dense particles	[123] [134]
	CNT	SWCNTs	Diameter of as-grown CNTs :0.8-1.2 nm	[124]
		MWCNTs	Length:200 μm (reaction time: 10 min) Diameter: 70-110 nm	[125]
	Sensor	SnO_2 gas sensors	Direct flame deposition High sensitivity and fast responses to NO_2 and propanal	[133]
	Phosphors	$Y_3Al_5O_{12}$: Ce	Mean size of the YAG : Ce phosphor powders: 1.73 μm Luminous intensity of white LED: 2.21 cd	[135]
	Glass frit	Silver powders coated with Pb-based glass material	Mean size of the composite powders: 42 nm Thickness of glass layer: 1.4 nm Sheet resistance: 19 mΩ/sq (sintering temp. 600 °C)	[108]
		Bi_2O_3-B_2O_3-ZnO-BaO-SiO_2 glass powders (Transparent dielectric layer in PDPs)	Transparencies of the dielectric layers: 94%	[77]
	Transistor	ZnO thin film	Demonstration of use of spray deposition process for preparing high-mobility and low-voltage ZnO transistor	[138]
		TiO_2 films	Deposition from solution by spray pyrolysis under ambient atmosphere. Maximum mobility value: 0.05 cm^2/V Air-stable operating characteristics with a shelf life time of several months	[139]
Bioceramics	Dental	Dental fillings (ceramic filler)	Diameter: 16 nm (with closely controlled refractive index, transparency, crystallinity) Production rate: 6.7-100 g/h	[96]
		Calcium phosphates (HAp)	Mean size of the BCP powders: 35 nm	[126]
	Bioceramics	Magnetic/luminescent core/shell particles	Narrow emission peak centred near 615 nm Demonstration of novel immunoassay format with internal luminescent calibration for more precise measurements	[127]

tially operated at low particle concentration compared to the liquid phase process.

In this review, we have discussed how researchers on spray pyrolysis overcome this inherent limitation of the aerosol process. In

the first part of this review, key criteria were explained for selecting each component of spray pyrolysis: precursor, additive, carrier gas, heat source, and reactor type. A mix-and-match of these elements would be a way of inventing a completely new spray pyrolysis process once product specifications are fixed. In the second part, key contributions of major groups in Korea, Japan, Europe, and America were mentioned. In the third part, some of named processes to overcome productivity of spray aerosol process were introduced. Especially, salt-assisted spray pyrolysis, emulsion-assisted spray pyrolysis, organic-assisted spray pyrolysis, low-pressure spray pyrolysis were discussed in detail. Finally, flexibility and applicability of spray pyrolysis were demonstrated by introducing various examples of applications to alternative energy, environmental cleaning, information processing and display, and biomaterials.

Here are some of standing issues for further progress in full scale commercial application and fundamental research. (1) In principle, the spray pyrolysis process produces one particle from one droplet. Therefore, it is important to understand the fundamental physics and chemistry occurring in one droplet when it is exposed to high temperature or low pressure. Especially, experimental observation of evaporation, precipitation and growth phenomena in one stagnant droplet will enhance understanding of particle formation in spray pyrolysis. Modeling of the growth process will be possible. (2) Spray pyrolysis is not an equilibrium process. It produces particles of meta-stable phase. Post heat treatment will drive the particles to a thermodynamically stable phase in segregated phase or homogeneous phase depending on phase diagram. Understanding the kinetics of this phase transformation process is another issue which has not been openly discussed so far. Coating or insertion of barrier materials, which slow down this process, should be investigated. (3) Large volume of gas and solvent involved in the process has to be cleaned and recycled. Minimization or optimization of gas and liquid is needed. New aerosol generation methods should be proposed in order to lower energy consumption. (4) More noble applications that only spray pyrolysis can produce should be discovered. Applications to health-related sensors and structures will be good application area. Mass production of transistor or LED by spray pyrolysis would be another example of noble applications of spray pyrolysis.

REFERENCES

1. Y. S. Chung, Y. C. Kang and S. B. Park, *J. Electrochem. Soc.*, **151**, H180 (2004).
2. M. E. Fortunato, M. Rostam-Abadi and K. S. Suslick, *Chem. Mater.*, **22**, 1610 (2010).
3. R. M. Laine, J. Marchal, H. Sun and X. Q. Pan, *Adv. Mater.*, **17**, 830 (2005).
4. B. J. Lokhande, P. S. Patil and M. D. Uplane, *Mater. Chem. Phys.*, **84**, 238 (2004).
5. H. Xu, L. Gao, H. Gu, J. Guo and D. Yan, *J. Am. Ceram. Soc.*, **85**, 139 (2002).
6. J. M. A. Caiut, J. Dexpert-Ghys, Y. Kihn, M. Verelst, H. Dexpert, S. J. L. Ribeiro and Y. Messaddeq, *Powder Technol.*, **190**, 95 (2009).
7. H. Chang, J.-H. Park and H. D. Jang, *Colloids Surf. A.*, **313**, 140 (2008).
8. H. N. Aiyer, S. Parashar, A. R. Raju, S. A. Shivashankar and C. N. R. Rao, *J. Phys. D.*, **32**, 1 (1999).
9. M. Jubault, J. Pulpytel, H. Cachet, L. Boufendi and F. Arefi-Khonsari, *Plasma Processes Polym.*, **4**, S330 (2007).
10. M. Nyman, J. Caruso and M. J. Hampden-smith, *J. Am. Ceram. Soc.*, **80**, 1231 (1997).
11. S. E. Skrabalak and K. S. Suslick, *J. Am. Chem. Soc.*, **127**, 9990 (2005).
12. Y. C. Kang, H. S. Roh and S. B. Park, *Adv. Mater.*, **12**, 451 (2000).
13. S. A. Song, K. Y. Jung and S. B. Park, *Langmuir*, **25**, 3402 (2009).
14. D. S. Jung, H. Y. Koo, H. C. Jang, J. H. Kim, Y. H. Cho, J.-H. Lee and Y. C. Kang, *J. Alloys Compd.*, **487**, 693 (2009).
15. C. P. Chan, H. Lam and C. Surya, *Sol. Energy Mater. Sol. Cells*, **94**, 207 (2010).
16. E. Reverchon and G. D. Porta, *Chem. Eng. Technol.*, **26**, 840 (2003).
17. D. S. Jung and Y. C. Kang, *J. Eur. Ceram. Soc.*, **28**, 2617 (2008).
18. T. Ogi, Y. Kaihatsu, F. Iskandar, E. Tanabe and K. Okuyama, *Adv. Powder Technol.*, **20**, 29 (2009).
19. L. Yuan, K. Konstantinov, G. X. Wang, H. K. Liu and S. X. Dou, *J. Power Sources*, **146**, 180 (2005).
20. F. Iskandar, S.-G. Kim, A. B. D. Nandiyanto, Y. Kaihatsu, T. Ogi and K. Okuyama, *J. Alloys Compd.*, **471**, 166 (2009).
21. D. Y. Kim, S. H. Ju, H. Y. Koo, S. K. Hong and Y. C. Kang, *J. Alloys Compd.*, **417**, 254 (2006).
22. D. S. Jung, S. K. Hong, S. H. Ju, H. J. Lee and Y. C. Kang, *Jpn. J. Appl. Phys. Part 1*, **44**, 4975 (2005).
23. H. Oh and S. Kim, *J. Aerosol Sci.*, **38**, 1185 (2007).
24. Y. C. Kang, H. S. Roh, S. B. Park and H. D. Park, *J. Eur. Ceram. Soc.*, **22**, 1661 (2002).
25. D. S. Jung, S. K. Hong, J. S. Cho and Y. C. Kang, *Mater. Res. Bull.*, **43**, 1789 (2008).
26. E. K. Nyutu, W. C. Conner, S. M. Auerbach, C. H. Chen and S. L. Suib, *J. Phys. Chem. C*, **112**, 1407 (2008).
27. J. C. Weigle, C. C. Luhrs, C. K. Chen, W. L. Perry, J. T. Mang, M. B. Nemer, G. P. Lopez and J. Phillips, *J. Phys. Chem. B*, **108**, 18601 (2004).
28. N. Kambe, *Scr. Mater.*, **44**, 1671 (2001).
29. D. S. Jung and Y. C. Kang, *Appl. Phys. A*, **94**, 411 (2009).
30. H. Y. Koo, J. H. Yi, Y. N. Ko, J. H. Kim and Y. C. Kang, *Powder Technol.*, **198**, 347 (2010).
31. D. A. Konopka, S. Pylypenko, P. Atanassov and T. L. Ward, *ACS Appl. Mater. Interfaces*, **2**, 86 (2010).
32. L. H. Song and S. B. Park, *J. Nanosci. Nanotechnol.*, **10**, 122 (2010).
33. S. S. Dunkle, R. J. Helmich and K. S. Suslick, *J. Phys. Chem. C*, **113**, 11980 (2009).
34. H. S. Roh, Y. C. Kang and S. B. Park, *J. Colloid Interface Sci.*, **228**, 195 (2000).
35. D. S. Jung, S. K. Hong, H. J. Lee and Y. C. Kang, *Opt. Mater.*, **28**, 530 (2006).
36. H. Y. Koo, S. H. Lee and Y. C. Kang, *Jpn. J. Appl. Phys.*, **47**, 7407 (2008).
37. Y. S. Chung, J. S. Lim, S. B. Park and K. Okuyama, *J. Chem. Eng. Jpn.*, **37**, 1099 (2004).
38. C. J. Brinker, Y. Lu, A. Sellinger and H. Fan, *Adv. Mater.*, **11**, 579 (1999).
39. J. S. Cho, D. S. Jung, S. K. Hong and Y. C. Kang, *J. Electroceram.*, **23**, 236 (2009).
40. M. J. Height, L. Madler, S. E. Pratsinis and F. Krumeich, *Chem.*

Mater., **18**, 572 (2006).
41. J. A. Azurdia, A. Mccrum and R. M. Laine, *J. Mater. Chem.*, **18**, 3249 (2008).
42. A. C. Sonavane, A. I. Inamdar, P. S. Shinde, H. P. Deshmukh, R. S. Patil and P. S. Patil, *J. Alloys Compd.*, **489**, 667 (2010).
43. D. S. Jung, H. Y. Koo and Y. C. Kang, *Colloids Surf. A*, **360**, 69 (2010).
44. J. H. Bang and K. S. Suslick, *Adv. Mater.*, **21**, 3186 (2009).
45. K. H. Lee, S. C. Rah and S.-G. Kim, *J. Sol-Gel Sci. Technol.*, **45**, 187 (2008).
46. H. Y. Koo, S. K. Hong, J. M. Han and Y. C. Kang, *J. Alloys Compd.*, **457**, 429 (2008).
47. S. H. Ju and Y. C. Kang, *Mater. Chem. Phys.*, **107**, 328 (2008).
48. H. S. Kang, Y. C. Kang, H. D. Park and Y. G. Shul, *Appl. Phys. A*, **80**, 347 (2005).
49. S. H. Ju, H. Y. Koo, D. Y. Kim, S. K. Hong, Y. C. Kang, H. W. Ha and K. Kim, *J. Mater. Sci. Mater. Electron.*, **17**, 353 (2006).
50. H. S. Roh, Y. C. Kang, H. D. Park and S. B. Park, *Appl. Phys. A*, **76**, 241 (2003).
51. H. Y. Koo, S. H. Ju, S. K. Hong, D. S. Jong, Y. C. Kang and K. Y. Jung, *Jpn. J. Appl. Phys.*, **45**, 9083 (2006).
52. K. Y. Jung, Y. C. Kang and Y.-K. Park, *J. Ind. Eng. Chem.*, **14**, 224 (2008).
53. H. Y. Koo, S. H. Ju, S. K. Hong, D. S. Jung, Y. C. Kang and K. Y. Jung, *Jpn. J. Appl. Phys. Part 1*, **45**, 9083 (2006).
54. D. S. Jung, S. K. Hong, S. H. Ju, H. Y. Koo and Y. C. Kang, *Jpn. J. Appl. Phys. Part 1*, **45**, 116 (2006).
55. G.-H. An, H.-J. Wang, B.-H. Kim, Y.-G. Jeong and Y.-H. Choa, *Mater. Sci. Eng. A*, **449**, 821 (2007).
56. C. Panatarani, I. W. Lenggoro and K. Okuyama, *J. Nanopart. Res.*, **5**, 47 (2003).
57. Y. Itoh and K. Okuyama, *J. Ceram. Soc. Jpn.*, **111**, 815 (2003).
58. Y. Itoh, I. W. Lenggoro, K. Okuyama, L. Madler and S. E. Pratsinis, *J. Nanopart. Res.*, **5**, 191 (2003).
59. K. K. Lee, Y. C. Kang, K. Y. Jung and J. H. Kim, *J. Alloys Compd.*, **395**, 280 (2005).
60. D. S. Jung, S. H. Lee and Y. C. Kang, *J. Ceram. Process. Res.*, **9**, 307 (2008).
61. D. S. Jung, H. Y. Koo, H. C. Jang and Y. C. Kang, *Met. Mater. Int.*, **15**, 809 (2009).
62. D. S. Jung and Y. C. Kang, *J. Magn. Magn. Mater.*, **321**, 619 (2009).
63. D. S. Jung, S. K. Hong, J. S. Cho and Y. C. Kang, *Mater. Res. Bull.*, **43**, 1789 (2008).
64. S. H. Ju, D. Y. Kim, H. Y. Koo, S. K. Hong, E. B. Jo and Y. C. Kang, *J. Alloys Compd.*, **425**, 411 (2006).
65. W. Widiyastuti, R. Balgis, F. Iskandar and K. Okuyama, *Chem. Eng. Sci.*, **65**, 1846 (2010).
66. T. Ogi, D. Hidayat, F. Iskandar, A. Purwanto and K. Okuyama, *Adv. Powder Technol.*, **20**, 203 (2009).
67. D. Hidayat, T. Ogi, F. Iskandar and K. Okuyama, *Mater. Sci. Eng.: B*, **151**, 231 (2008).
68. I. W. Lenggoro, Y. Itoh, N. Iida and K. Okuyama, *Mater. Res. Bull.*, **38**, 1819 (2003).
69. W. H. Suh and K. S. Suslick, *J. Am. Chem. Soc.*, **127**, 12007 (2005).
70. S.-H. Hu, G.-H. Cheng, M.-Y. Cheng, B.-J. Hwang and R. Santhanam, *J. Power Sources*, **188**, 564 (2009).
71. K. C. Pingali, S. Deng and D. A. Rockstraw, *Powder Technol.*, **183**, 282 (2008).
72. R. Strobel, F. Krumeich, W. J. Stark, S. E. Pratsinis and A. Baiker, *J. Catal.*, 222, 307 (2004).
73. H. W. Kang and S. B. Park, *Adv. Powder Technol.*, 21, 106 (2010).
74. D. J. Seo, K. O. Ryu, S. B. Park, K. Y. Kim and R.-H. Song, *Mater. Res. Bull.*, **41**, 359 (2006).
75. Y. S. Chung, S. B. Park and D.-W. Kang, *Mater. Chem. Phys.*, **86**, 375 (2004).
76. J. S. Cho, Y. N. Ko, H. Y. Koo and Y. C. Kang, *J. Mater. Sci. Mater. Med.*, **21**, 1143 (2010).
77. S. K. Hong, H. Y. Koo, D. S. Jung, I. S. Suh and Y. C. Kang, *J. Alloys Compd.*, **437**, 215 (2007).
78. S. H. Lee, H. Y. Koo, D. S. Jung, J. M. Han and Y. C. Kang, *Opt. Mater.*, **31**, 870 (2009).
79. S. H. Ju and Y. C. Kang, *J. Power Sources*, **195**, 4327 (2010).
80. S. H. Ju and Y. C. Kang, *J. Power Sources*, **178**, 387 (2008).
81. J. H. Yi, H. Y. Koo, J. H. Kim, Y. N. Ko, Y. C. Kang, H. M. Lee and J. Y. Yun, *J. Alloys Compd.*, **490**, 488 (2010).
82. H. D. Jang, H. K. Chang, H. S. Yoon, K. Cho, J. H. Park and S. Y. Oh, *Colloids Surf. A*, **313**, 121 (2008).
83. K. Cho, H. Chang, J. H. Park, B. G. Kim and H. D. Jang, *J. Ind. Eng. Chem.*, **14**, 860 (2008).
84. H. Chang, S. J. Kim, H. D. Jang and J. W. Choi, *Colloids Surf. A*, **313**, 282 (2008).
85. H. D. Jang, C. M. Seong, H. K. Chang and H. C. Kim, *Curr. Appl. Phys.*, **6**, 1044 (2006).
86. H. Chang, I. W. Lenggoro, K. Okuyama and H. D. Jang, *Jpn J. Appl. Phys.*, **45**, 967 (2006).
87. H. D. Jang, C. M. Seong, Y. J. Suh, H. C. Kim and C. K. Lee, *Aerosol Sci. Technol.*, **38**, 1027 (2004).
88. C. S. Kim, E. K. Park and S.-G. Kim, *J. Sol-Gel Sci. Technol.*, **47**, 7 (2008).
89. H.-S. Kim, K.-H. Lee and S.-G. Kim, *Aerosol Sci. Technol.*, **40**, 536 (2006).
90. H.-S. Kim, C. S. Kim and S.-G. Kim, *J. Non-Cryst. Solids*, **352**, 2204 (2006).
91. D.-J. Kang, S.-G. Kim and H.-S. Kim, *J. Mater. Sci.*, **39**, 5719 (2004).
92. R. Kubrin, A. Tricoli, A. Camenzind, S. E. Pratsinis and W. Bauhofer, *Nanotechnol.*, **21**, 225603 (2010).
93. T. J. Patey, R. Buchel, S. H. Ng, F. Krumeich, S. E. Pratsinis and P. Novak, *J. Power Sources*, **189**, 149 (2009).
94. W. J. Stark, L. Madler, M. Maciejewski, S. E. Pratsinis and A. Baiker, *Chem. Commun.*, **2003**, 588 (2003).
95. R. Strobel, S. E. Pratsinis and A. Baiker, *J. Mater. Chem.*, **15**, 605 (2005).
96. H. Schulz, L. Madler, S. E. Pratsinis, P. Burtscher and N. Moszner, *Adv. Funct. Mater.*, **15**, 830 (2005).
97. A. Tricoli, M. Righettoni and S. E. Pratsinis, *Langmuir*, **25**, 12578 (2009).
98. B. J. Lokhande, P. S. Patil and M. D. Uplane, *Mater. Lett.*, **57**, 573 (2002).
99. P. S. Patil, R. K. Kawar, S. B. Sadale and P. S. Chigare, *Thin Solid Films*, **437**, 34 (2003).
100. S. R. Bathe and P. S. Patil, *Sol. Energy Mater. Sol. Cells*, **91**, 1097 (2007).
101. A. V. Moholkar, S. M. Pawar, K. Y. Rajpure, S. N. Almari, P. S. Patil and C. H. Bhosale, *Sol. Energy Mater. Sol. Cells*, **92**, 1439

(2008).
102. J. H. Bang, R. J. Hehnich and K. S. Suslick, *Adv. Mater.*, **20**, 2599 (2008).
103. S. E. Skrabalak and K. S. Suslick, *J. Phys. Chem.*, **111**, 17807 (2007).
104. M. Kim and R. M. Laine, *J. Am. Ceram. Soc.*, **93**, 709 (2010).
105. B. Weidenhof, M. Reiser, K. Stowe, W. F. Maier, M. Kim, J. Azurdia, E. Gulari, E. Seker, A. Barks and R. M. Laine, *J. Am. Chem. Soc.*, **131**, 9207 (2009).
106. T. R. Hinklin and R. M. Laine, *Chem. Mater.*, **20**, 553 (2008).
107. R. M. Laine, J. C. Marchal, H. P. Sun and X. Q. Pan, *Nature Mater.*, **5**, 710 (2006).
108. J. Marchal, T. John, R. Baranwal, T. Hinklin and R. M. Laine, *Chem. Mater.*, **16**, 822 (2004).
109. A. B. D. Nandiyanto, Y. Kaihatsu, F. Iskandar and K. Okuyama, *Mater. Lett.*, **63**, 1847 (2009).
110. Y. Terashi, A. Purwanto, W.-N. Wang, F. Iskandar and K. Okuyama, *J. Eur. Ceram. Soc.*, **28**, 2573 (2008).
111. W.-N. Wang, Y. Itoh, I. W. Lenggoro and K. Okuyama, *Mater. Sci. Eng.: B*, **111**, 69 (2004).
112. H. Chang, I. W. Lenggoro, T. Ogi and K. Okuyama, *Mater. Lett.*, **59**, 1183 (2005).
113. K. Myojin, T. Ogihara, N. Ogata, N. Aoyagi, H. Aikiyo, T. Ookawa, S. Omura, M. Yanagimoto, M. Uede and T. Oohara, *Adv. Powder Technol.*, **15**, 397 (2004).
114. T. Ogihara, H. Aikiyo, N. Ogata, K. Katayama, Y. Azuma, H. Okabe and T. Okawa, *Adv. Powder Technol.*, **13**, 437 (2002).
115. H. Yamada, T. Okawa, T. Ogihara and N. Ogata, *Jpn. J. Appl. Phys.*, **45**, 7475 (2006).
116. I. Taniguchi, K. Matsuda, H. Furubayashi and S. Nakajima, *AIChE J.*, **52**, 2413 (2006).
117. I. Taniguchi, S. Nakajima and Z. Bakenov, *Chem. Eng. Commun.*, **195**, 1292 (2008).
118. S. Suda, K. Kawahara, M. Kawano, H. Yoshida and T. Inagaki, *J. Am. Ceram. Soc.*, **90**, 1094 (2007).
119. S. Ohara, R. Maric, X. Zhang, K. Mukai, T. Fukui, H. Yoshida, T. Inagaki and K. Miura, *J. Power Sources*, **86**, 455 (2000).
120. R. A. Afre, T. Soga, T. Jimbo, M. Kumar, Y. Ando and M. Sharon, *Chem. Phys. Lett.*, **414**, 6 (2005).
121. S. H. Ju, H. C. Jang and Y. C. Kang, *J. Power Sources*, **189**, 163 (2009).
122. H. S. Kang, J. R. Sohn, Y. C. Kang, K. Y. Jung and S. B. Park, *J. Alloys Compd.*, **398**, 240 (2005).
123. B. Xia, I. W. Lenggoro and K. Okuyama, *J. Am. Ceram. Soc.*, **84**, 1425 (2001).
124. I. Khatri, T. Soga, T. Jimbo, S. Adhikari, H. R. Aryal and M. Umeno, *Diamond Relat. Mater.*, **18**, 319 (2009).
125. A. Aguilar-Elguezabal, W. Antunez, G. Alonso, F. P. Delgado, F. Espinosa and M. Miki-Yoshida, *Diamond Relat. Mater.*, **15**, 1329 (2006).
126. R. S. Kalubarme, M. B. Kadam and S. H. Pawar, *J. Alloys Compd.*, **479**, 732 (2009).
127. D. Dosev, M. Nichkova, R. K. Dumas, S. J. Gee, B. D. Hammock, K. Liu and I. M. Kennedy, *Nanotechnol.*, **18** (2007).
128. S. K. Hong, D. S. Jung and Y. C. Kang, *J. Electroceram.*, **23**, 437 (2009).
129. Y. C. Kang and S. B. Park, *J. Aerosol Sci.*, **26**, 1131 (1995).
130. Y. C. Kang, S. B. Park and Y. W. Kang, *Nanostructured Mater.*, **5**, 777 (1995).
131. B. Xia, W. Lenggoro and K. Okuyama, *Adv. Mater.*, **13**, (2001).
132. R. Strobel and S. E. Pratsinis, *J. Mater. Chem.*, **17**, 4743 (2007).
133. R. Strobel, J. D. Grunwaldt, A. Camenzind and S. E. Pratsinis, *Catal. Lett.*, **104**, 1 (2005).
134. W. N. Wang, Y. Itoh, I. W. Lenggoro and K. Okuyama, *Mater. Sci. Eng. B*, **111**, 69 (2004).
135. S. H. Lee, D. S. Jung, J. M. Han, H. Y. Koo and Y. C. Kang, *J. Alloys Compd.*, **477**, 776 (2009).
136. Y. C. Kang, K. Y. Jung and S. B. Park, *Korean Chem. Eng. Res.*, **44**, 235 (2006).
137. K. Y. Koo and S. B. Park, *J. Am. Ceram. Soc.*, **90**, 3736 (2007).
138. A. Bashir, P. H. Wobkenberg, J. Smith, J. M. Ball, G. Adamopoulos, D. D. C. Bradley, T. D. Anthopoulous, *Adv. Mater.*, **21**, 2226 (2009).
139. P. H. Wöbkenberg, T. Ishwara, J. Nelson, D. D. C. Bradley, S. A. Haque and T. D. Anthopoulos, *Appl. Phys. Lett.*, **96**, 082116 (2010).
140. Z. Wu, M. Okuya and S. Kaneko, *Thin Solid Films*, **385**, 109 (2001).
141. Y. J. Lee, H. B. Kim and Y. R. Roh, *Jpn. A. Appl. Phys.*, **40**, 2423 (2001).
142. S. H. Park, S. W. Oh and Y. K. Su, *J. Power Sources*, **146**, 622 (2005).
143. S. H. Park, S. W. Oh, S. H. Kang, I. Belharouak, K. Amine and Y. K. Sun, *Electrochim. Acta*, **52**, 7227 (2007).
144. S. Aoyagi, Y. Kuroiwa, A. Sawada, H. Kawaji and T. Atake, *Therm. Anal. Calorim.*, **81**, 627 (2005).
145. J. H. Bang, K. K. Han, S. E. Skrbalak, H. S. and Kim and K. S. Suslick, *J. Phys. Chem.*, **111**, 10959 (2007).
146. S. W. Jung, Y. C. Kang and J. H. Kim, *J. Mater. Sci.*, **42**, 9783 (2007).
147. D. S. Jung, S. H. Lee and Y. C. Kang, *Opt. Mater.*, **30**, 1810 (2008).
148. S. H. Ju, S. K. Hong, H. C. Jang and Y. C. Kang, *J. Ceram. Soc. Jpn.*, **115**, 507 (2007).
149. S. H. Ju and Y. C. Kang, *Mater. Res. Bull.*, **43**, 590 (2008).
150. W. N. Wang, Y. Itoh, I. W. Lenggoro and K. Okuyama, *Mater. Sci. Eng. B*, **111**, 69 (2004).
151. W. N. Wang, I. W. Lenggoro and Y. Terashi, *J. Mater. Res.*, **20**, 2873 (2005).
152. Y. Itoh, M. Abdullah and K. Okuyama, *J. Mater. Res.*, **19**, 1077 (2004).
153. H. Y. Koo, S. K. Hong, S. H. Ju and Y. C. Kang, *J. Non-Cryst. Solids*, **352**, 3270 (2006).
154. S. Gamburzev, A. J. Appleby, K. Kunze, P. Atanassova, P. Atanassov, M. H. Smith and T. Kodas, The Proceedings of 197th ECS meeting, Toronto (2000).
155. J. Y. Rim, S. A. Song and S. B. Park, *Mat. Res. Soc. Symp. Proc.*, **703** (2002).
156. T. T. Kodas and M. H. Smith, Aerosol Processing of materials, Wiley-VCH, New York (1999).
157. T. T. Kodas, A. Sood and S. E. Pratsinis, *Powder Technol.*, **50**, 47 (1987).
158. H. Y. Koo, J. H. Yi, J. H. Kim, Y. K. Yun and Y. C. Kang, *Colloids Surf. A*, **361**, 45 (2010).